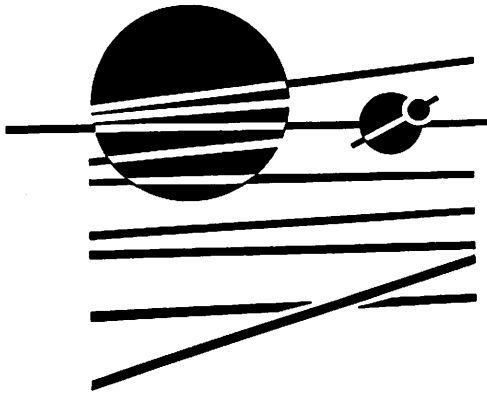

Lunar and Planetary Laboratory
Department of Planetary Sciences

White Mountains and Canyon de Chelly

Planetary Geology Field Practicum
PTYS 594a
October 11-13, 2003

The University of Arizona
Tucson, Arizona

Table of Contents

White Mountains and Canyon de Chelly
Planetary Geology Field Practicum
PTYS 594a
October 11-13, 2003

Itinerary
PtyS 594a - Fall 2003
White Mountains & Canyon de Chelly

Friday - October 10

Drivers pick up vehicles from UA Motor Pool
Drivers pick up radios and road emergency kits from Gould-Simpson locker

Saturday - October 11

7:30 am	Load vehicles at the LPL loading dock.
8:00 am	Vehicles begin rolling (earlier if possible) Cherry to Speedway, left on Speedway. Speedway to Stone, right on Stone. Stone to Drachman, left on Drachman. Drachman to Oracle, right on Oracle Continue on Oracle, which will become State Route 77. At Oracle Junction, bear right to continue on SR 77. At Globe, continue on SR 77 & US Route 60 At Show Low, take SR 260 towards Pinetop-Lakeside
12:30 pm	Lunch near Show Low; if we made good time, we will have lunch between Show Low and Pinetop-Lakeside at the Mogollon Rim Nature Trail. (If we did not make good time, we will have lunch before we reach Show Low at a point north of the Fort Apache Indian Reservation. Subsequent times in today's itinerary will then be 1 to 1½ hours later than listed.)
1:00 pm	Vehicles begin rolling again; driving into White Mountains. At Hon Dah, continue (go left) on SR 260 towards McNary Radio presentation (to be augmented later, if necessary): Glacial history of the White Mountains: Jani R. Turn right onto SR 273; follow until it transitions into Forest Road 113 Continue on FR 113 until we reach the Mt. Baldy Trailhead
2:30 pm	Mt. Baldy trailhead; begin hike (bring extra layer of clothing and flashlight, along with normal amount of snack food, water, and field guides). Ideally, we will hike approximately 2.75 miles (5.5 miles roundtrip) where several moraines are located. Presentations during hike today or in the morning: Glaciers and glaciation (types of glaciers, conditions needed for formation): David O. Glacial deposits: Celinda M. Glacial erosional features: Curtis C. Periglacial processes and features: Abby S. Global climate cycles over the past million years: Carl H.

6:30 pm — Set up camp
Primary site: at end of FR 554
Backup sites exist along FR 113, FR 112, and SR 373

Sunday - October 12

7:30 am — Clean camp site; break camp.

8:00 am — Vehicles are rolling

Radio presentation (to be augmented later, if necessary):

Where is the sky blue? — Jason B.

12:30 pm — Lunch in the Chinle area, ideally in the Canyon de Chelly National Monument Visitors' Center: Check-in for the evening's campsite, to ensure gate is unlocked.

1:15 pm — Begin rim tours (north and south) in vehicles, stopping where appropriate for sapping features and presentations.

Presentations to be made during rim tours:

Geology & stratigraphy of the Colorado Plateau and the Canyon de Chelly region:	Tamara G.
Sapping processes and landforms in Arizona:	Jim R.
Sapping landforms on other solar system bodies:	Oleg A.
Crossbedding and implications for climate:	John M.
Atmospheric convection over the desert:	Joe S.

6:00 pm — Set up camp at Canyon de Chelly group campsite #1.

Monday - October 13

7:30 am — Clean camp site; break camp.

8:00 am — Vehicles are rolling

Option 1: White Ruins hike at Canyon de Chelly
Option 2: Investigate Petrified National Park (additional fee)
(Note: all vehicles will stay together.)

12:00 pm — Lunch, location dependent on the morning's option

12:45 pm — Begin return to Tucson, if not already en route.
I-40 west to Flagstaff.
I-17 south to Phoenix.
I-10 east to Tucson; exit Speedway and return to LPL.

5:30 - 7:30 — Arrive at LPL, time depending on morning's option

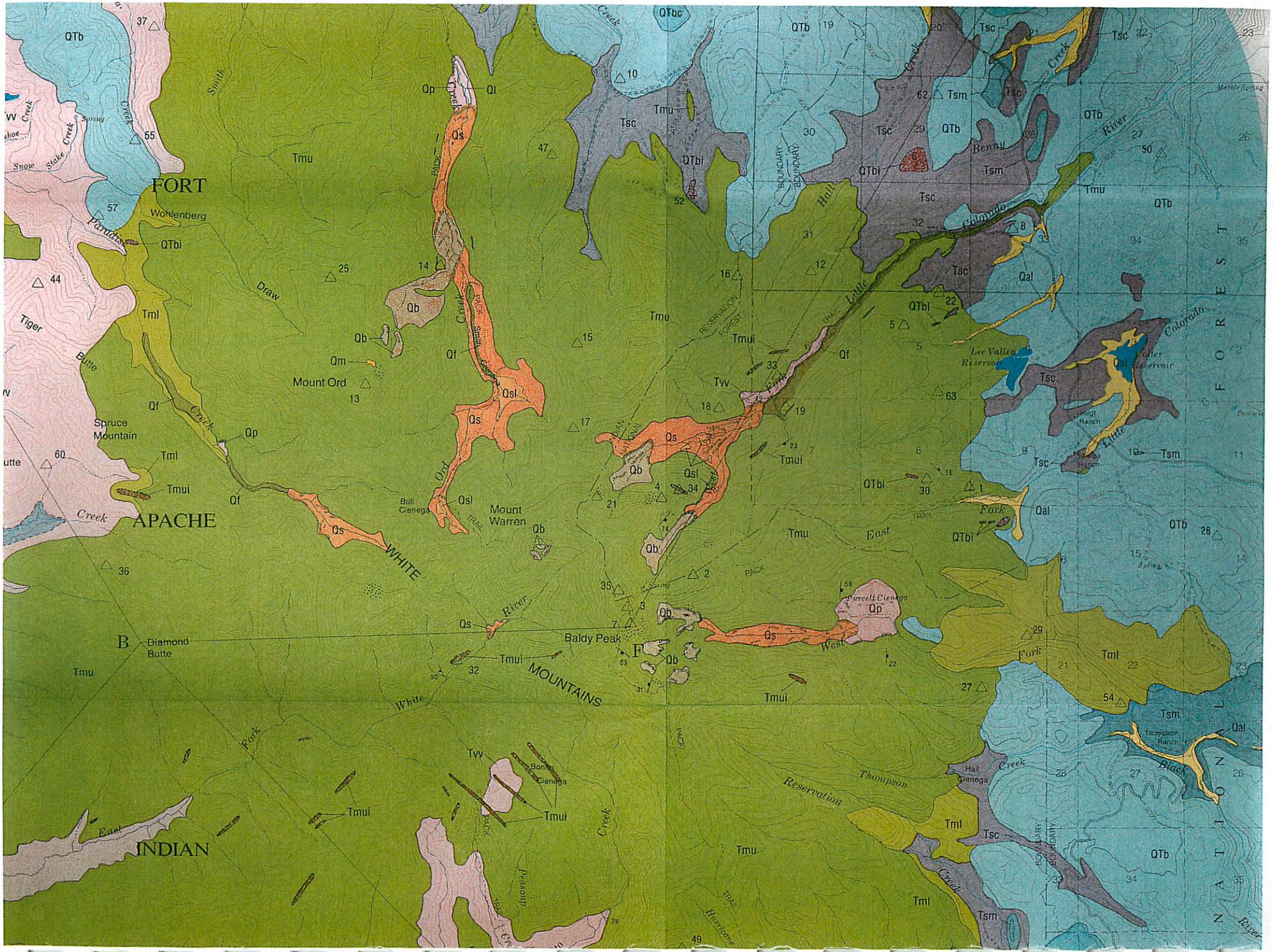
FORT
Wohlenberg
APACHE
INDIAN
Spruce Mountain
Mount Ord
Mount Warren
Diamond Butte
Baldy Peak
MOUNTAINS
Tiger
Butte
Creek
Draw
Smith
Paradise
Snow Stake Creek
Spring
Bull Cienega
Bonita Cienega
Purcell Cienega
Hall Cienega
Thompson Ranch
Lee Valley Reservoir
Colorado
Little
Black
River
White
East
West
Fork
Reservation
BOUNDARY
TRAIL
PACK
FOREST
NATIONAL
QTb
QTbc
QTbi
Tml
Tmu
Tmui
Tsc
Tsm
Tvy
Qal
Qb
Qf
Qm
Qp
Qs
Qsl
Ql

Route for Fall '03 Field trip

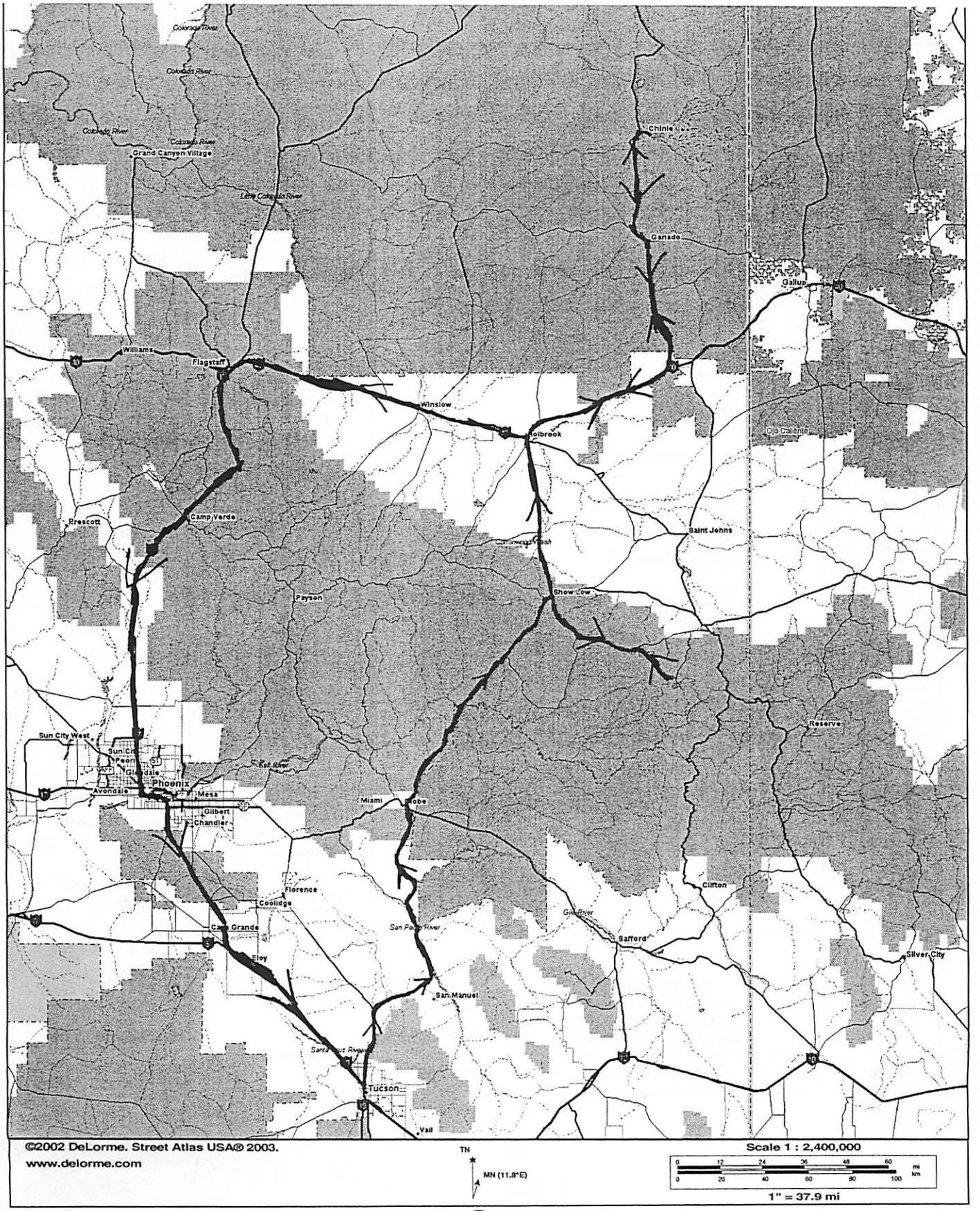

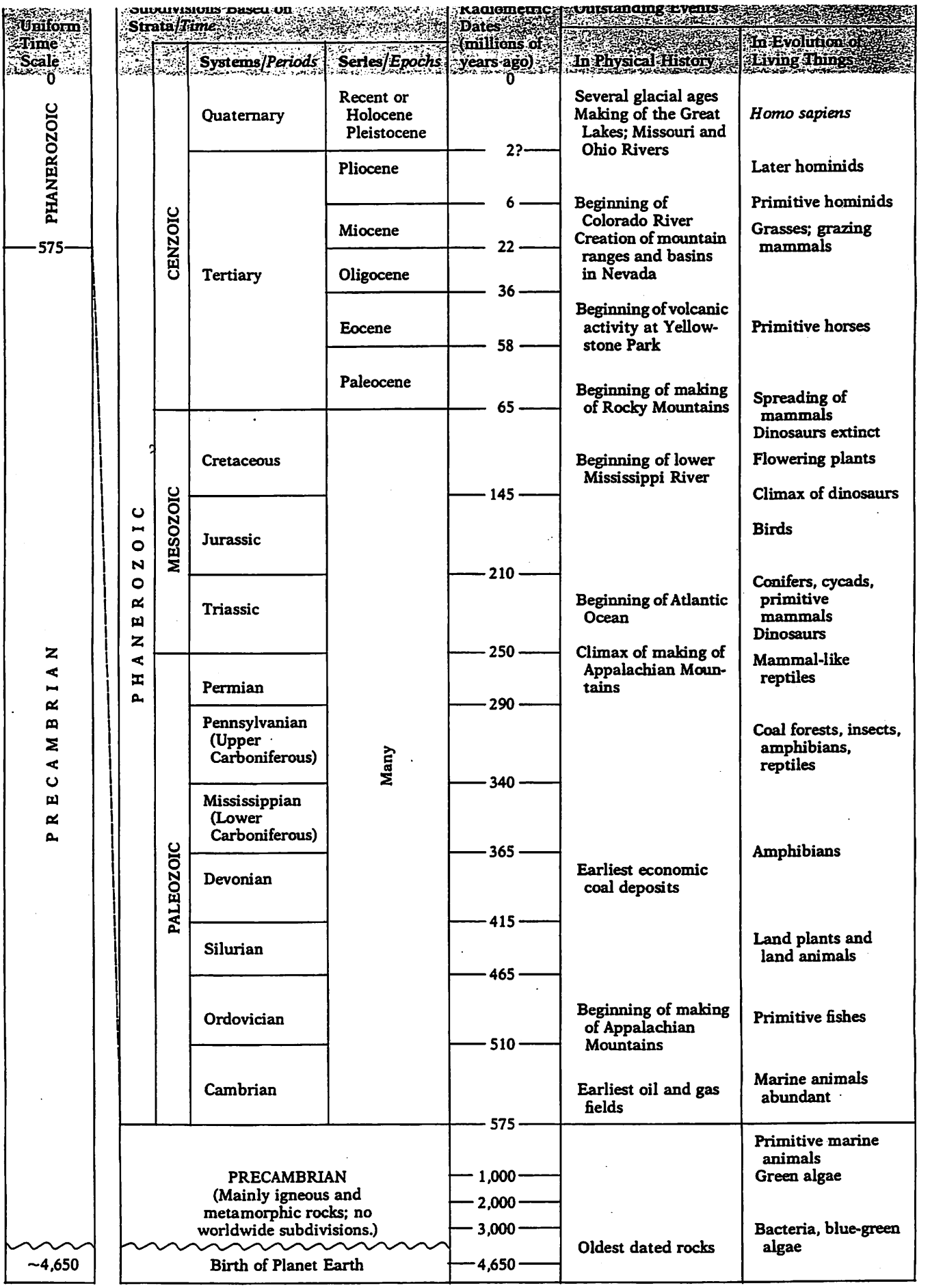

Flint & Skinner, "Physical Geology" 2 ed (1977)

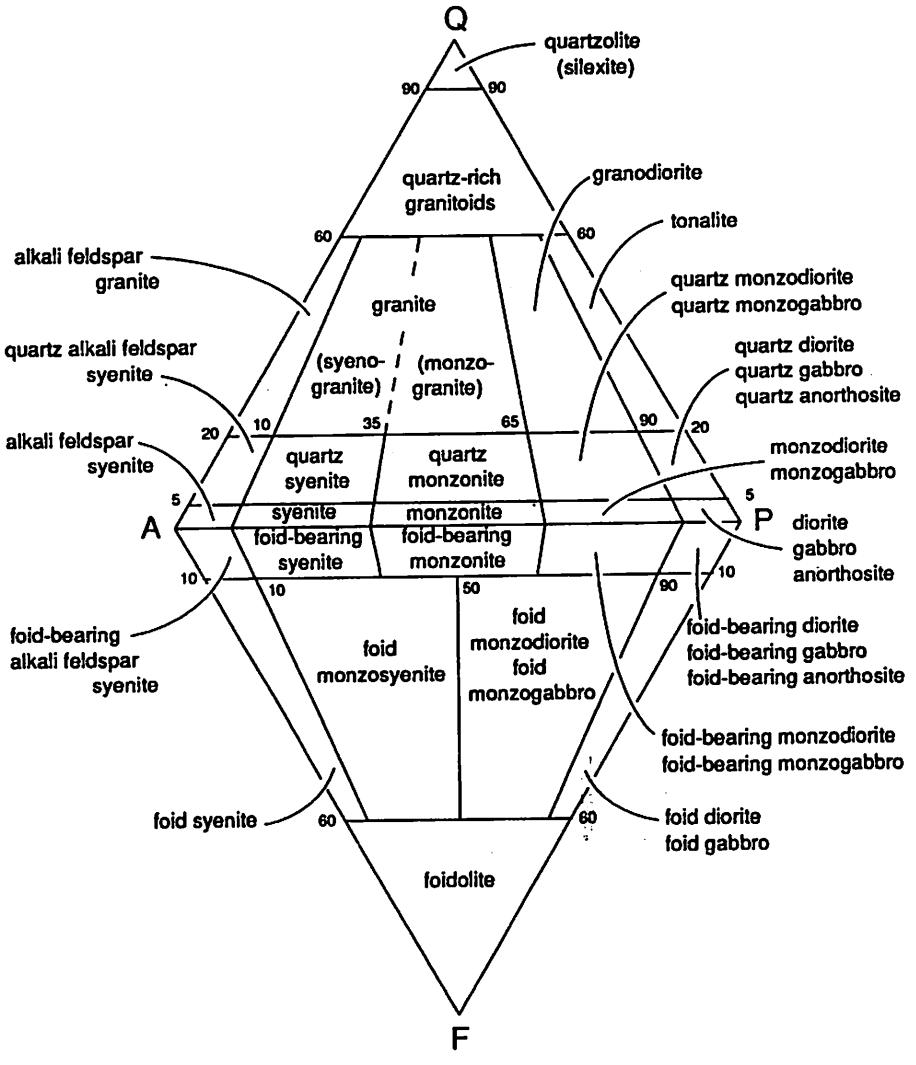

Fig. B.4. Classification and nomenclature of plutonic rocks according to their modal mineral contents using the QAPF diagram (based on Streckeisen, 1976, Fig. 1a). The corners of the double triangle are Q = quartz, A = alkali feldspar, P = plagioclase and F = feldspathoid. However, for more detailed definitions refer to section B.2. This diagram must not be used for rocks in which the mafic mineral content, M, is greater than 90%.

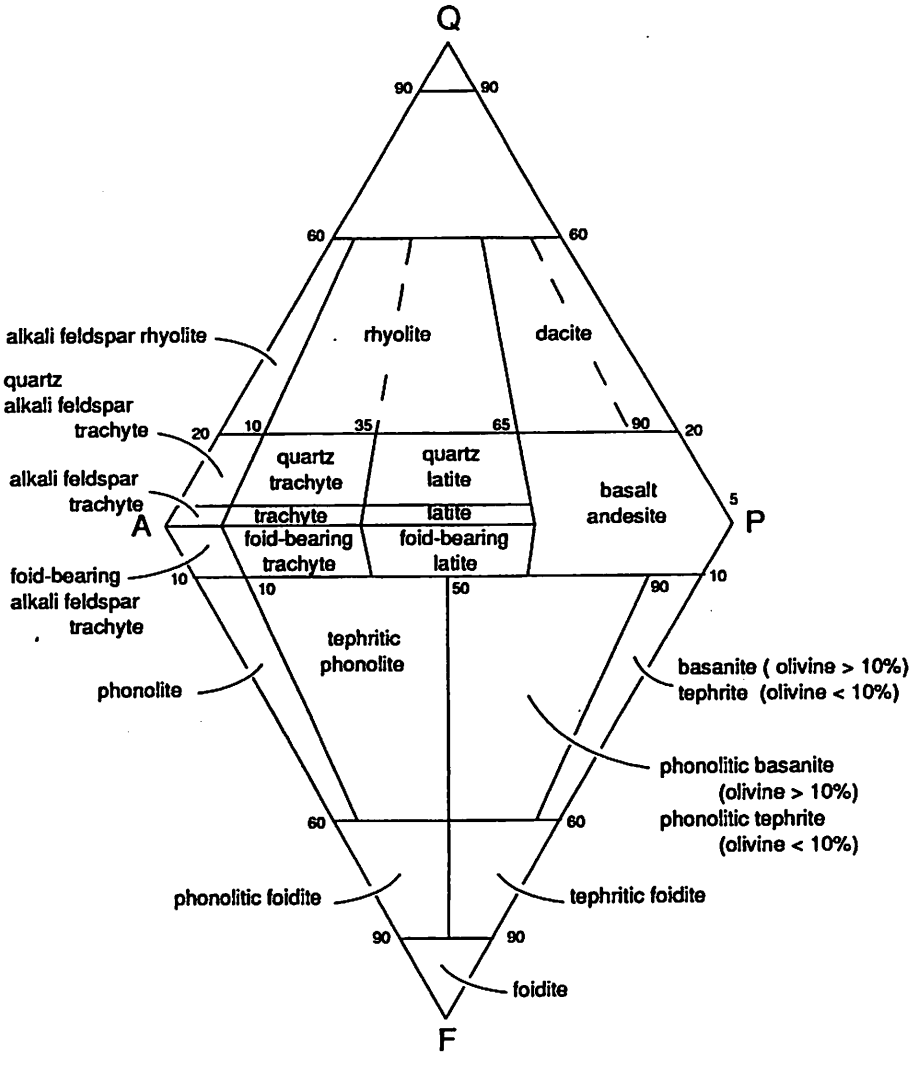

Fig. B.10. Classification and nomenclature of volcanic rocks according to their modal mineral contents using the QAPF diagram (based on Streckeisen, 1978, Fig. 1). The corners of the double triangle are Q = quartz, A = alkali feldspar, P = plagioclase and F = feldspathoid. However, for more detailed definitions refer to section B.2.

5

"Classification of Igneous Rocks and Glossary of Terms" Le Maitre, ed. Blackwell Scientific Publications (1989)

TABLE 7-3 Classification of Chemical and Biochemical Sedimentary Rocks

Texture	Composition	Rock Name	
Clastic or crystalline	Calcite ($CaCO_3$)	Limestone (includes coquina, chalk, and oolitic limestone)	Carbonates
	Dolomite [$CaMg(CO_3)_2$]	Dolostone	
Crystalline	Gypsum ($CaSO_4 \cdot 2H_2O$)	Rock gypsum	Evaporites
	Halite (NaCl)	Rock salt	
Usually crystalline	Microscopic SiO_2 shells	Chert	
—	Altered plant remains	Coal	

TABLE 7-2 Classification of Detrital Sedimentary Rocks

Sediment Name and Size	Description	Rock Name	
Gravel (>2 mm)	Rounded gravel	Conglomerate	
	Angular gravel	Sedimentary breccia	
Sand (1/16–2 mm)	Mostly quartz	Quartz sandstone	
	Quartz with >25% feldspar	Arkose	
Mud (<1/16 mm)	Mostly silt	Siltstone	Mudrocks
	Silt and clay	Mudstone*	
	Mostly clay	Claystone*	

*Mudrocks possessing the property of fissility, meaning they break along closely spaced, parallel planes, are commonly called *shale*.

FIGURE 7-9 (*a*) Photomicrograph of a sandstone showing a clastic texture consisting of fragments of minerals, mostly quartz in this case. (*b*) Photomicrograph of the crystalline texture of a limestone showing a mosaic of calcite crystals.

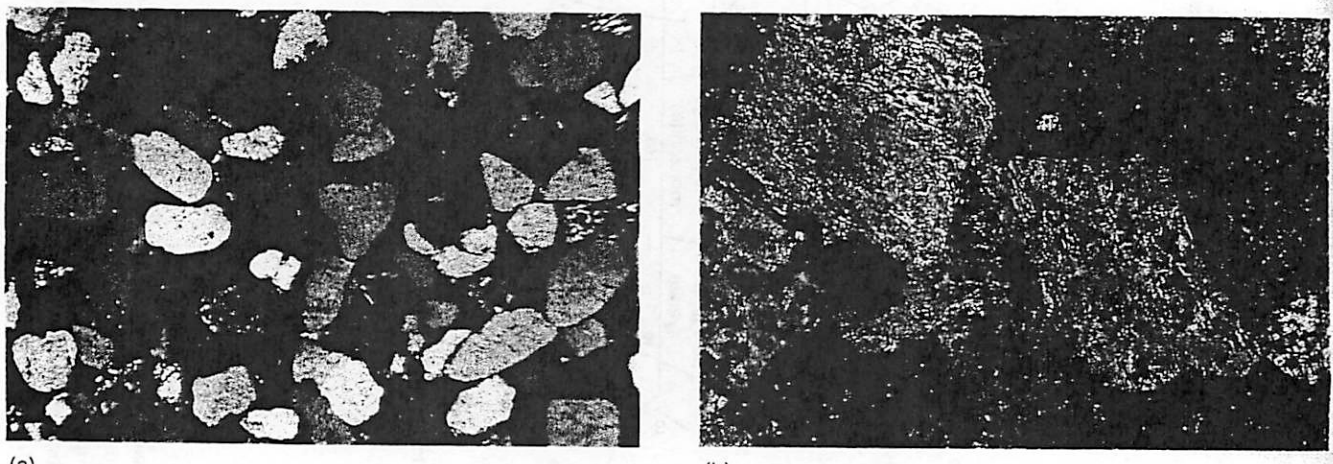

(a) (b)

from Physical Geology
Monroe + Wicander (1992)

6

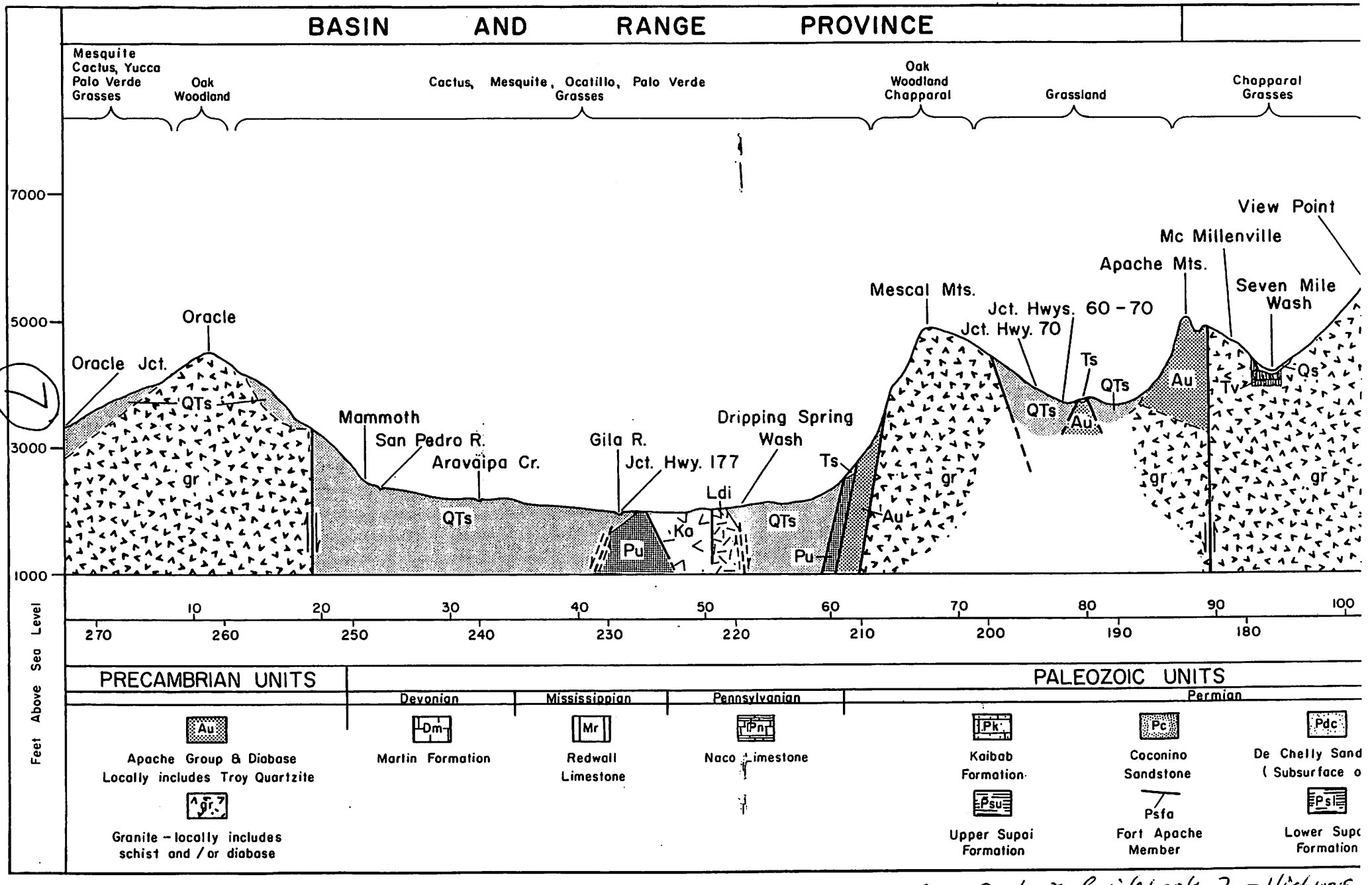

Figure 4. Profile and section along Arizona Highway 77 showing principal rock units, geographic features, and vegetative types. View looking westerly.

From PEIRCE, H.W., 1971, Geologic Guidebook 2 - Highways of Arizona, AZ Hwys 77 & 177, AZ Bureau of Mines, Bulletin 176, Univ. of Ariz., Tucson, AZ.

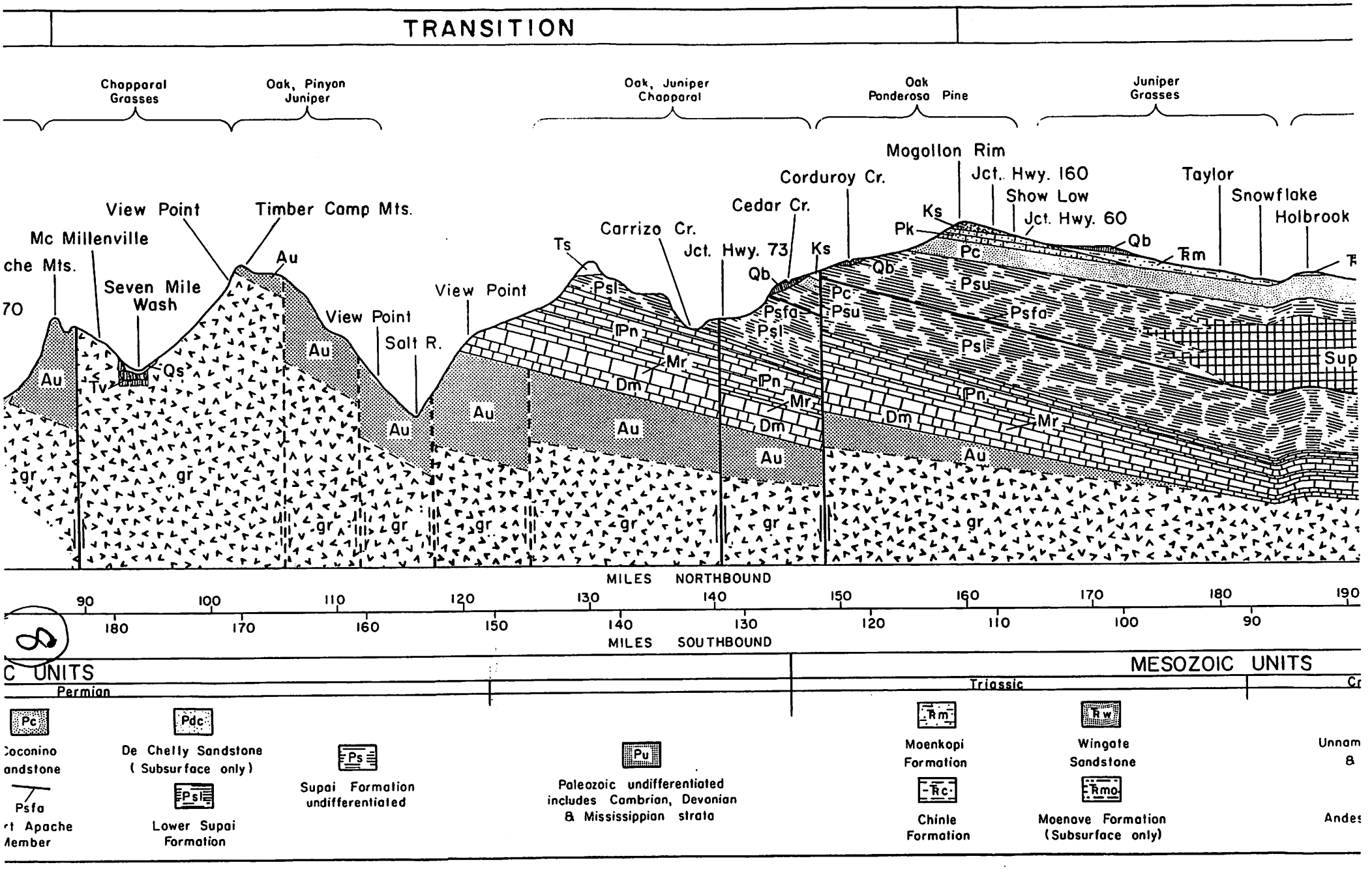
TRANSITION
Chapparal Grasses
Oak, Pinyon Juniper
Oak, Juniper Chapparal
Oak Ponderosa Pine
Juniper Grasses
Mogollon Rim
Corduroy Cr.
Jct. Hwy. 160
Show Low
Jct. Hwy. 60
Taylor
Snowflake
Holbrook
Cedar Cr.
Carrizo Cr.
Jct. Hwy. 73
View Point
Timber Camp Mts.
Mc Millenville
Seven Mile Wash
Salt R.
Ts
Ks
Pk
Qb
Pc
Psu
Psfa
Psl
Pn
Mr
Dm
Au
Tv
Qs
Tm
Sup
gr
MILES NORTHBOUND
90 100 110 120 130 140 150 160 170 180 190
180 170 160 150 140 130 120 110 100 90
MILES SOUTHBOUND
PALEOZOIC UNITS
Permian
Triassic
MESOZOIC UNITS
Pc
Coconino Sandstone
Psfa
Apache Member
Pdc
De Chelly Sandstone (Subsurface only)
Psl
Lower Supai Formation
Ps
Supai Formation undifferentiated
Pu
Paleozoic undifferentiated includes Cambrian, Devonian & Mississippian strata
Rm
Moenkopi Formation
Rc
Chinle Formation
Rw
Wingate Sandstone
Rmo
Moenave Formation (Subsurface only)
Unnam
Andes

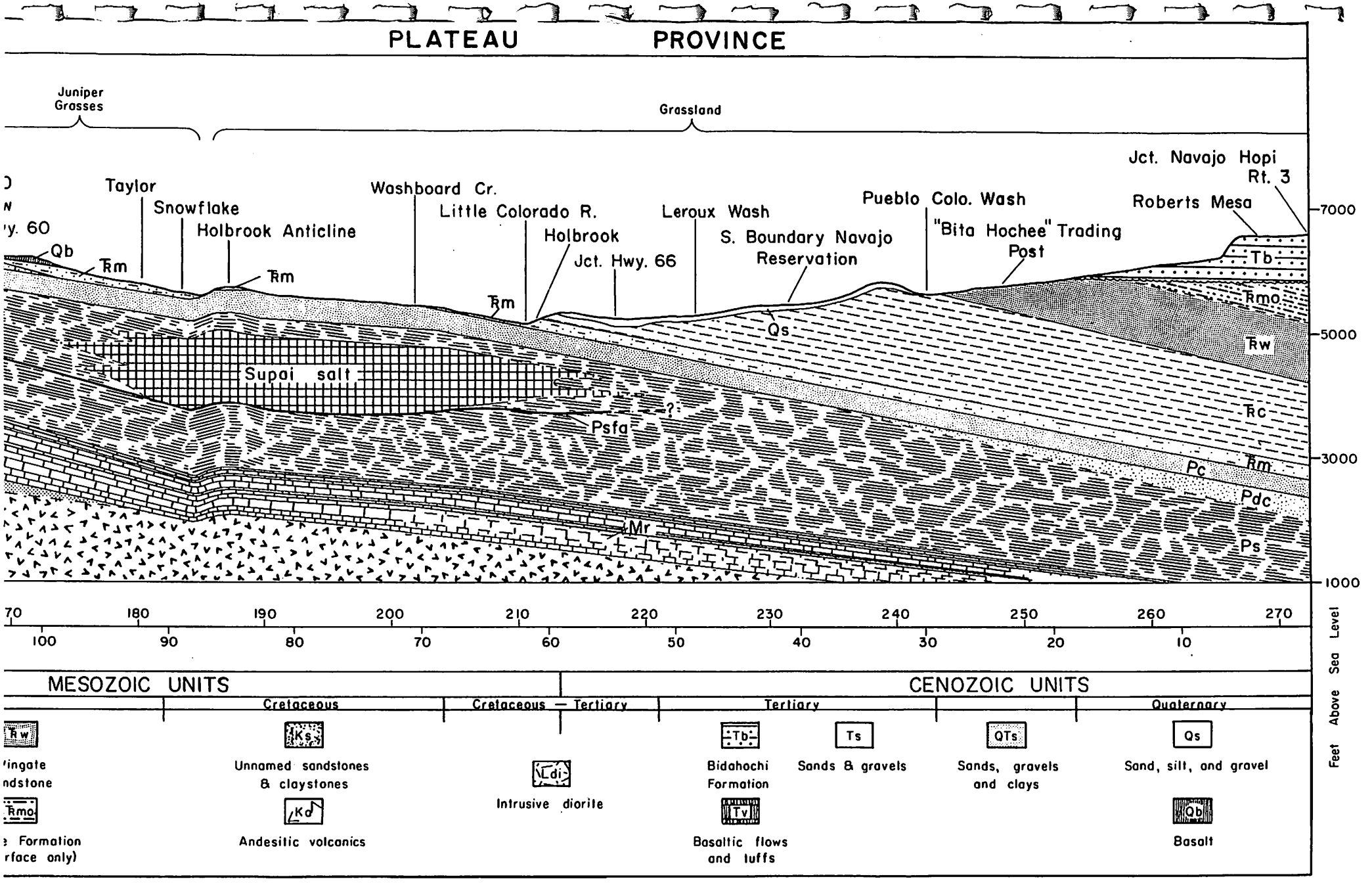
PLATEAU PROVINCE
Juniper Grasses
Grassland
Taylor
Snowflake
Holbrook Anticline
Washboard Cr.
Little Colorado R.
Holbrook
Jct. Hwy. 66
Leroux Wash
S. Boundary Navajo Reservation
Pueblo Colo. Wash
"Bita Hochee" Trading Post
Jct. Navajo Hopi Rt. 3
Roberts Mesa
Qb
Rm
Supai salt
Psfa
Qs
Tb
Rmo
Rw
Rc
Pc
Pdc
Ps
Mr
7000
5000
3000
1000
Feet Above Sea Level
MESOZOIC UNITS
CENOZOIC UNITS
Cretaceous
Cretaceous — Tertiary
Tertiary
Quaternary
Unnamed sandstones & claystones
Intrusive diorite
Bidahochi Formation
Sands & gravels
Sands, gravels and clays
Sand, silt, and gravel
Andesitic volcanics
Basaltic flows and tuffs
Basalt

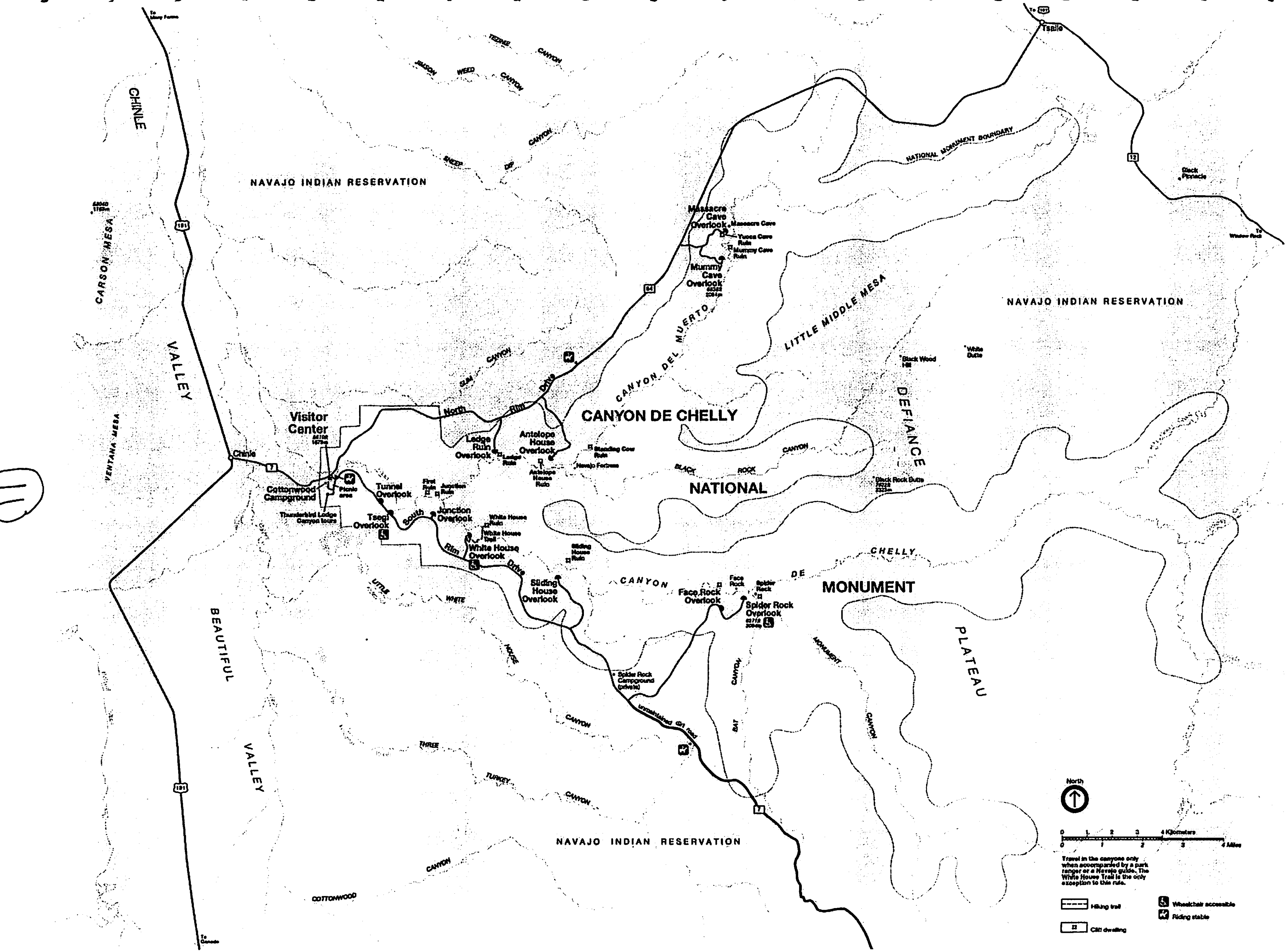
CANYON DE CHELLY
NATIONAL
MONUMENT
NAVAJO INDIAN RESERVATION
NAVAJO INDIAN RESERVATION
NAVAJO INDIAN RESERVATION
DEFIANCE
PLATEAU
LITTLE MIDDLE MESA
CANYON DEL MUERTO
CANYON DE CHELLY
CHINLE
VALLEY
BEAUTIFUL
VALLEY
CARSON MESA
VENTANA MESA
NATIONAL MONUMENT BOUNDARY
Visitor Center
Chinle
Tsaile
Cottonwood Campground
Thunderbird Lodge Canyon tours
Picnic area
Tunnel Overlook
Tsegi Overlook
Junction Overlook
White House Overlook
White House Ruin
White House Trail
Sliding House Overlook
Sliding House Ruin
Face Rock Overlook
Face Rock
Spider Rock Overlook
Spider Rock
Spider Rock Campground (private)
Ledge Ruin Overlook
Ledge Ruin
Antelope House Overlook
Antelope House Ruin
Standing Cow Ruin
Navajo Fortress
First Ruin
Junction Ruin
Massacre Cave Overlook
Massacre Cave
Yucca Cave Ruin
Mummy Cave Ruin
Mummy Cave Overlook
North Rim Drive
South Rim Drive
unestablished dirt road
Black Rock Butte
Black Wood Hill
White Butte
Black Pinnacle
BLACK ROCK CANYON
MONUMENT CANYON
BAT CANYON
WHITE HOUSE CANYON
LITTLE WHITE
THREE TURKEY CANYON
COTTONWOOD CANYON
SHEEP DIP CANYON
JAUSON WEED CANYON
TEZNIE CANYON
SUM CANYON
To Many Farms
To Ganado
To Window Rock
North
0 1 2 3 4 Kilometers
0 1 2 3 4 Miles
Travel in the canyons only when accompanied by a park ranger or a Navajo guide. The White House Trail is the only exception to this rule.
Hiking trail
Cliff dwelling
Wheelchair accessible
Riding stable

11

Grant, 1978

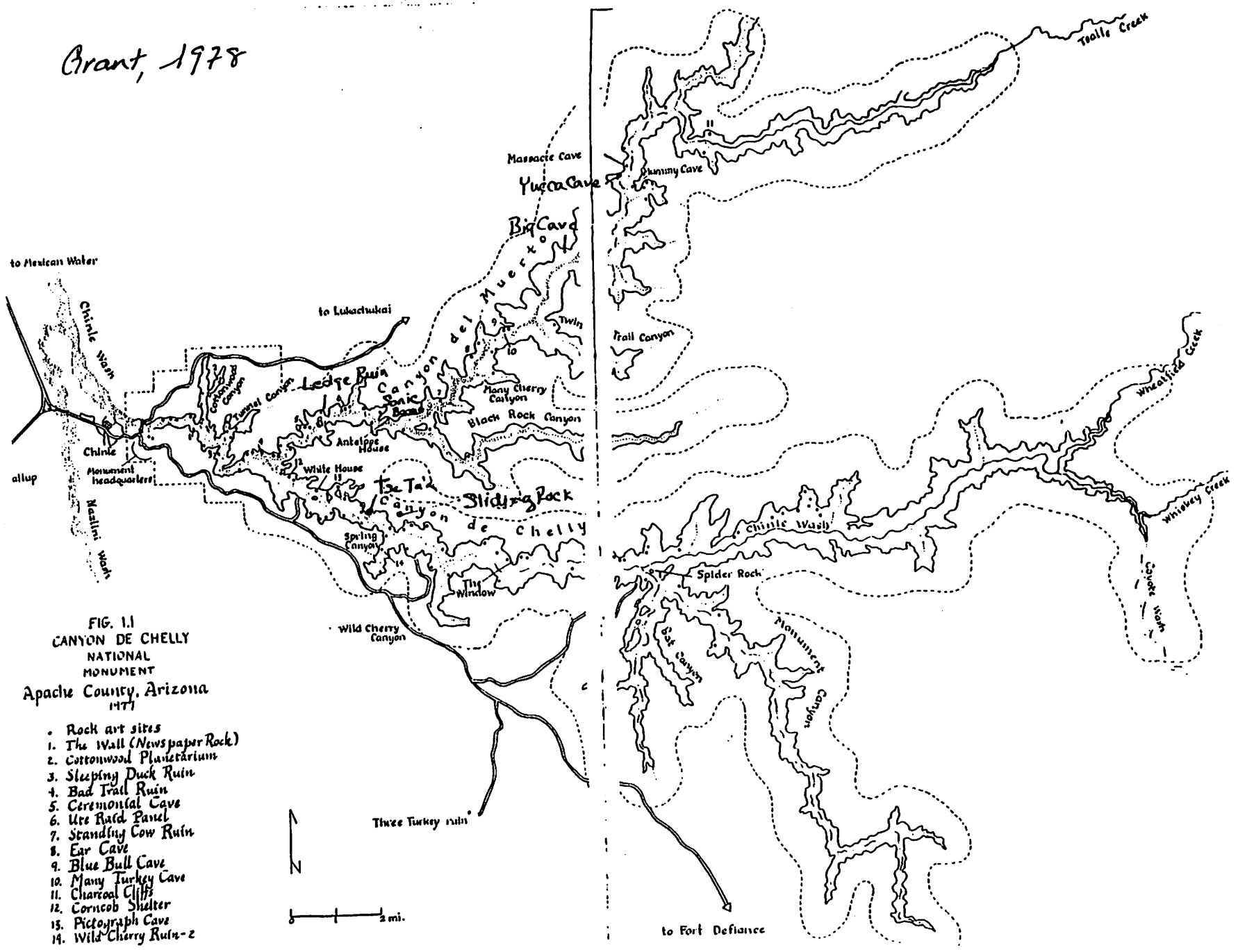

FIG. 1.1
CANYON DE CHELLY
NATIONAL
MONUMENT
Apache County, Arizona
1977

- Rock art sites
1. The Wall (Newspaper Rock)
2. Cottonwood Planetarium
3. Sleeping Duck Ruin
4. Bad Trail Ruin
5. Ceremonial Cave
6. Ute Raid Panel
7. Standing Cow Ruin
8. Ear Cave
9. Blue Bull Cave
10. Many Turkey Cave
11. Charcoal Cliffs
12. Corncob Shelter
13. Pictograph Cave
14. Wild Cherry Ruin-2

Cenozoic Geologic History (mostly glacial) of the White Mountains, Arizona

Jani Radebaugh

We could go into great detail about the Precambrian deformation belts that underlie the crust of central Arizona, or the many transgressions and regressions of the continental interior seaways of the Paleozoic and the Mesozoic that built up the layers so spectacularly exposed in the Grand Canyon to the northwest. For the most part, we'll be standing on top of all of this, however, so here we'll just talk about the outcrops and deposits of the late Cenozoic, or the time period from about 9 million years ago to the present. The glacial features are of the most interest for our trip, but we must discuss the geology upon which glaciers acted in order to get a feel for the overall setting.

Volcanism

The surprisingly high 11,403 foot **Mt. Baldy**, as well as nearby Mt. Ord and other surrounding peaks are all made of middle Tertiary (Miocene) **latite** (similar to andesite, only more potassium-rich) and quartz latite lava flows. They erupted about 8.6 +- 0.4 million years ago in a large, broad, **stratovolcano** (like Mt. St. Helens or other Cascades volcanoes) that likely reached 13,000 feet or more in elevation upon eruption. These lava flows are moderately **silica rich**, and are therefore quite viscous. This leads to the high, cone-like shape to the edifice, as lavas do not flow to great distances from the source. These lavas have high total alkalis and appear to be from a deep-reservoir magma brought up in a tensional tectonic environment, similar to the San Francisco mountains. As we are on the edge of the **Basin and Range** province, this is a likely scenario.

This eroded stratovolcano is surrounded by the **White Mountains Volcanic Field**, a Quaternary (several hundred thousand years old) lava flow field of **basalts** and basaltic cinder cones, again similar to the San Francisco volcanic field.

Glaciation

Earth entered several successive cooling time periods (see Karl's presentation) accompanied by increased precipitation in this region (as much as 20-25% more) that led to glaciation. Glaciers (=**MOVING ice**) persist if: 1-Supply is sufficient to feed the top of the glacier and 2-Melting is not sufficient enough to get rid of the ice in the summer. These conditions are easier to achieve if there is high elevation, hence there was extensive glaciation on the ancestral volcanic peak of the present day White Mountains.

Four main periods of glaciation occurred in this area, three during the Pleistocene, beginning about 65,000 years ago, and the last one in the Holocene, just 3,000 years ago. The specific dates and glacial features are listed in the table. This region is one of the southernmost places where alpine glaciers, or those carving out the tops of mountains, can be found. This glaciation leads to very specific geomorphology, in the form of spine-like **aretes, cirques**, and **horns** (Celinda will talk more about these).

Could we recognize these features on the mountains of other planets? On Io, where there appears to be a steady supply of SO2 frost, has this led to erosion of high peaks through SO2 "glaciation"?

Period	Epoch	Glacial Epoch	Local Glaciation	Glacial Features	Volcanism	Age
Quaternary	Holocene		Mt. Ord	moraines in high valleys		3 ka
	Pleistocene	Late-Wisconsinan	Baldy Peak	sharp-crested moraines	White Mountain Volcanic Field: basalt flows and cinder cones	10 ka
		Wisconsinan	Smith Cienega	moraines, fluvial and lacustrine deposits		
		Pre-Wisconsinan	Purcell	U-shaped valleys, moraines		>65 ka
Tertiary	Miocene				Mt. Baldy Volcanic Suite: latite, quartz latite, alkali-rich lava flows	8.6 ma

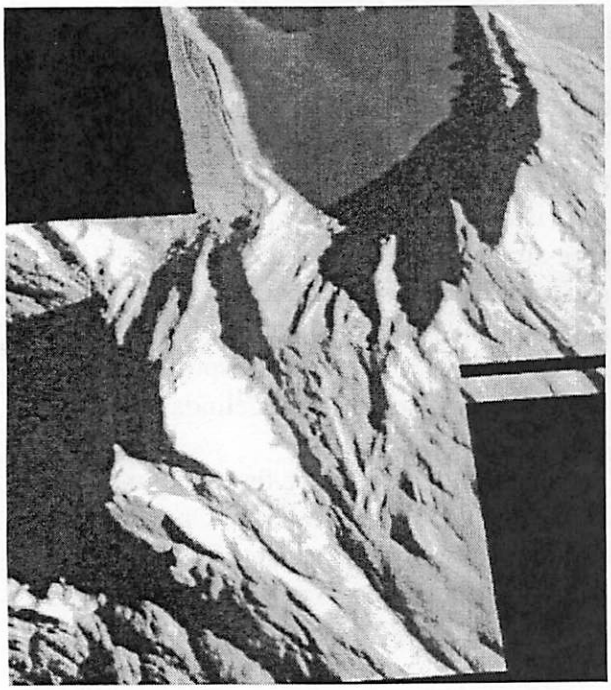

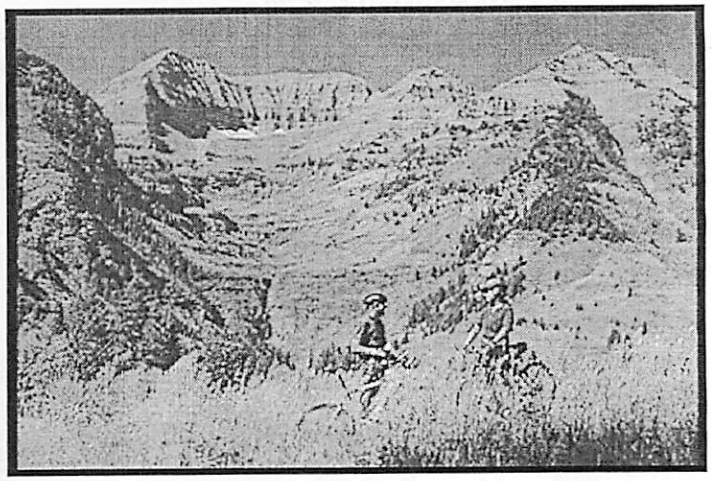

Glacial cirques and aretes at Mt. Timpanogos, Utah (picture from http://www.offroadpub.com)

Tohil Mons and Patera, Io. The mountain rises 6 km above the surrounding plains. Illumination is from the right. Brightness contrasts could be due to varying amounts of SO2 frosts. Image ~60 km across, resolution 50 m/pixel. From http://pirlwww.lpl.arizona.edu

References: Merrill, R. K. and T. L. Pewe, Late Cenozoic Geology of the White Mountains, Arizona, State of Arizona Bureau of Geology and Mineral Technology Special Paper No. 1, University of Arizona, 1977.
Wicander, R. and J. S. Monroe, Historical Geology, West Publishing Co., St. Paul, MN, 1993.
Colorado Plateau Land Use: http://www.cpluhna.nau.edu

Glaciers: How They Form and How They Move

Dave O'Brien

1 Introduction

Glaciers come is a range of forms, from continent-covering 'ice sheets' such as the Antarctic and Greenland ice sheets to smaller, more localized mountain glaciers, often termed 'ice streams.' All glaciers form where ice accumulates (generally from compacted snow) and then flows downslope (usually slower than a meter per day) where it is melted away, calved away as icebergs, or otherwise wasted away. Glaciers may advance and retreat due to climactic changes, but can be relatively stable over timescales of hundreds of thousands to millions of years or more, with ice production, flow, and wasting being roughly in balance.

2 Ice Formation and Removal

The primary source of glacial ice is snowfall, although the crystallization of atmospheric water vapor can play a minor role. Large amounts of snowfall are not required—small amounts of snowfall in areas where there is little or no melting, such as the Antarctic, still form massive glaciers. Over many seasons, this snowfall builds up layer upon layer, such that the lowest layers experience significant pressure. The initially fluffy, finely crystalline snow is compacted to form large single crystals which can be as 10 cm or more in diameter. If some meltwater is present, as in lower latitude glaciers, the snow-ice transition can occur only 10 m or so below the surface. In much colder glaciers, such as the Greenland and Antarctic ice sheets, the transition may be 60 m or more below the surface. Mountain glaciers often begin in a bowl-shaped area where snow accumulates, then feeds into smaller ice streams. The upper region of a glacier where the generation of new ice exceeds the removal of ice is termed the 'accumulation zone.'

In the lower portion of a glacier, termed the 'ablation zone,' the rate of removal of ice exceeds the generation rate of new ice. The ice can be removed by a number of means,

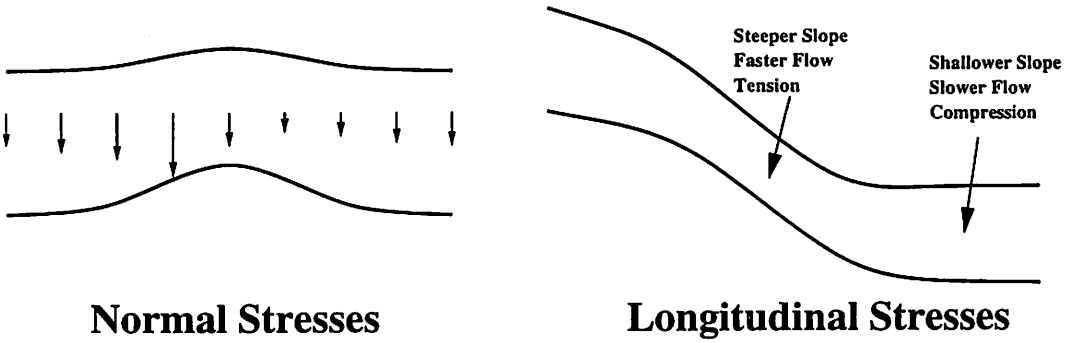

Figure 1: Diagram showing localized normal and longitudinal stress concentrations in a glacier due to changes in subsurface topography.

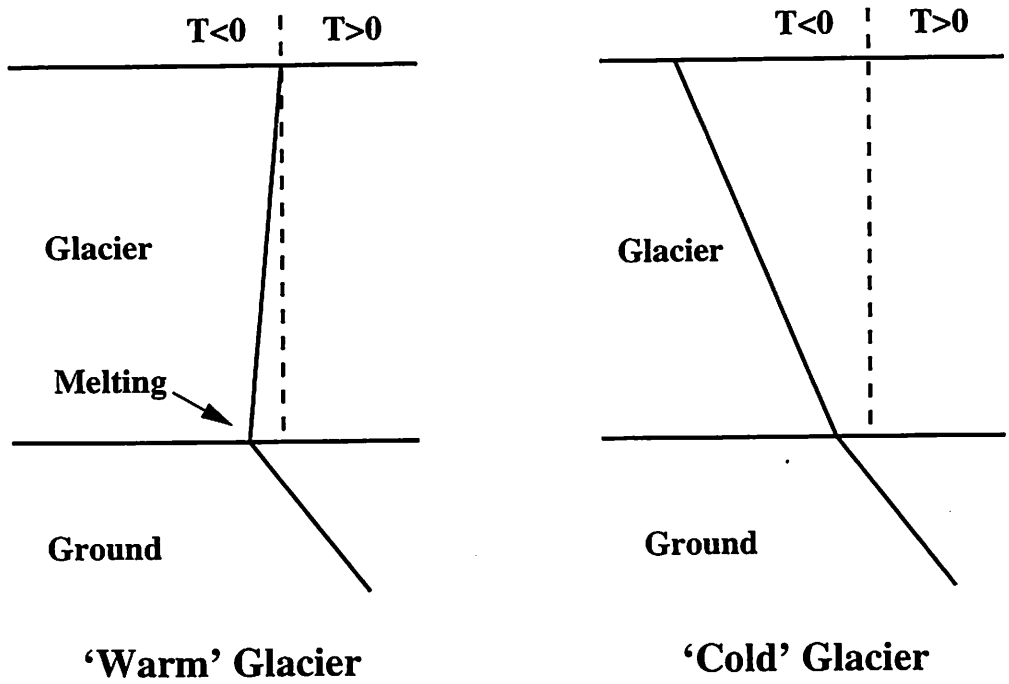

Figure 2: Idealized temperature profiles in 'warm' and 'cold' glaciers. Note that the temperature profile of a warm glacier allows for basal melting, while that of a cold glacier does not.

primarily melting and 'calving.' Calving occurs where a glacier enters the sea or a lake and chunks of it break off. Melting can be caused by solar radiation, as well as by rainfall or the condensation of water vapor (releasing latent heat). Wind can increase the rate of ice ablation by melting and/or sublimation due to warm and/or dry air being blown over the glacier.

3 Stress and Strain in Glaciers

The average normal and shear stresses at the base of a glacier (for small slopes) are given by

$$\sigma_b = \rho g h \tag{1}$$

$$\tau_b = \rho g h \sin\theta \tag{2}$$

where h is the glacier thickness and θ is the slope of the glacier. In a steady state, the basal shear stress must be resisted by opposing stresses from the channel that the glacier is flowing through (for ice streams) or the surface it's flowing over (for ice sheets). The thicker the glacier, the larger the normal and shear stresses. The steeper the glacier, the larger the shear stress.

There can be local stresses superimposed on these average stresses. Local normal stresses can result from topography on the surface the glacier flows over. For example, a glacier flowing over a bump will first experience an increase in basal normal stress as it runs into the bump, then a decrease once it passes the bump (Fig. 1). Such changes in normal stress can affect the patterns of deposition and erosion by the glacier.

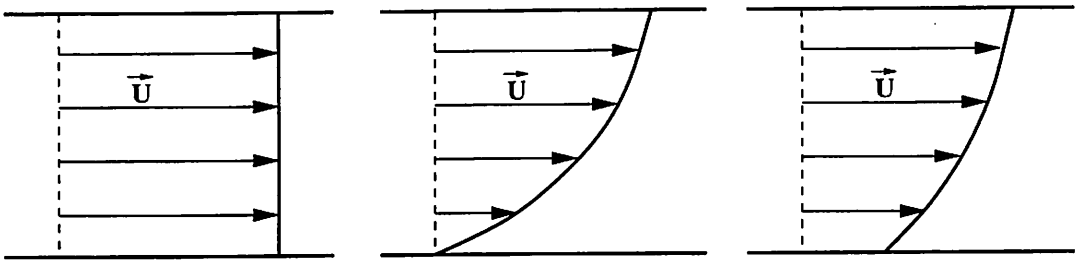

Figure 3: Diagram showing the vertical velocity profiles associated with pure basal sliding, pure internal deformation, and a combination of both of these processes. The arrows indicate the flow direction and velocity U, and the upper and lower lines are the upper and lower surface of the glacier

Local longitudinal stresses (along the direction of flow) can result from changes in the slope of a glacier (Fig. 1). If the slope increases, the glacier will thin and be in tension. If the slope decreases, the glacier will thicken and be in compression. Tensional stresses can lead to the formation of crevasses in the glacier.

The strain rate of glacier ice in response to shear stress is generally described by the non-Newtonian relation known as Glen's Flow Law

$$\dot{\epsilon} = A\tau^n \tag{3}$$

where n is generally close to 3 and A is strongly temperature dependent (A $\sim 10^{-17}$ at -40° C and 10^{-14} at 0° C). However, the actual flow law may differ depending on the bulk orientation of the ice crystals in the glacier, the presence of impurities, or the dominance of different creep mechanisms.

4 Temperature Profiles in Glaciers

At a depth of about 1,500 m, the melting point of ice is -1° C. For a glacier which is at the melting point everywhere along its depth, this means that there will be a positive upwards thermal gradient, and heat can not be conducted upwards. Because of this, there is generally some 'basal melting' due to geothermal heat which is trapped. Such glaciers are termed 'warm' or 'temperate' glaciers, and most glaciers in all but the coldest areas fall into this category. In places such as Greenland and Antarctica, the surface temperature of glaciers can be -40° C or lower, giving a negative thermal gradient capable of conducting away the geothermal heat flux, such that there is no basal melting. Such glaciers are termed 'cold' or 'polar' glaciers. If a cold glacier thickens at some point, it may no longer be able to conduct the geothermal heat away and some basal melting could then occur. Figure 2 shows idealized temperature profiles in these two types of glaciers. The difference in temperature and the presence of basal melting has important consequences for the mobility of these two types of glaciers, as will be discussed later.

5 Mass Movement and Flow Profiles In Glaciers

Glaciers flow downslope at generally less than a meter per day. There are two main process by which glaciers move—internal deformation and basal sliding. In the case of pure internal

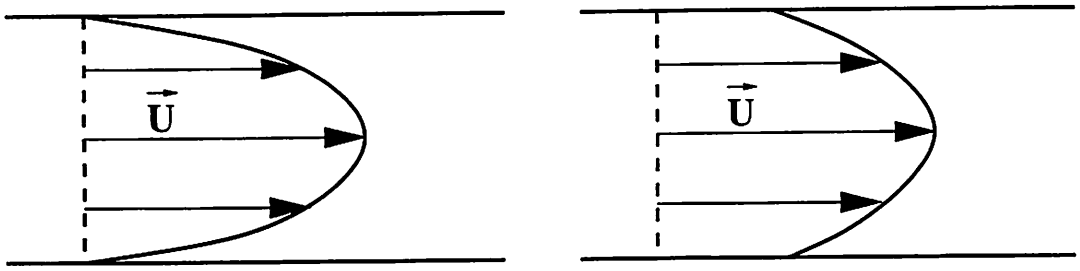

Figure 4: Diagram showing the velocity profiles across a glacier flowing through a channel for the case of no slip along the sides and some slip along the sides. Both cases have internal deformation. The arrows indicate the flow direction and velocity U

deformation, the base of a glacier is locked to the surface it flows over (and for confined ice streams, the sides of the glacier are locked to the walls of the channel it flows through), and the glacier itself flows in response to the driving stresses. In pure basal sliding, the glacier slides along the surface it flows over, or the basal sediments themselves deform, but the glacier does not deform internally. For a confined ice stream, the glacier would slide past the walls of the channel as well. In general, the actual motion of a glacier is a combination of internal deformation and basal sliding. Basal sliding can lead to frictional heating that may be comparable to the geothermal heat flow. Possible vertical velocity profiles are shown in Fig. 3, and possible velocity profiles across the surface of a confined ice stream are shown in Fig. 4 If the surface over which a glacier flows is very irregular, the velocity profile across the surface of a glacier may not be symmetrical.

'Warm' glaciers experience basal melting and generally some surface melting that can percolate down to the base through crevasses. This water can lubricate the base of the glacier allowing it to slip over the base of the channel and/or saturate the basal sediments thus allowing those sediments to deform more easily. In addition, the warmer ice can deform much more easily than cold ice. Cold, polar glaciers such as those in Greenland and Antarctica generally experience little or no basal melting and little or no melting on the surface, and their colder temperatures lead to significantly lower internal deformation. Thus, cold glaciers generally move much more slowly than warm glaciers.

Glaciers (almost always warm glaciers) can sometimes 'surge,' or experience sudden large movements of tens of meters or more per day for periods of weeks or months. Most surges have been studied long after they occurred, but for the few that have been studied as they were occurring, nearly all of their motion is due to basal sliding, most likely aided by water.

6 References:

Benn, D. I. and Evans, D. J. A. 1998. Glaciers and Glaciation. Wiley and Sons, NY.

Sharp, R. P. 1988. Living Ice: Understanding Glaciers and Glaciation. Cambridge University Press, NY.

Van Der Veen, C. J. 1999. Fundamentals of Glacier Dynamics. A. A. Balkema, Rotterdam.

Glacial Deposits

Celinda Marsh

All sedimentary material deposited as the result of glacial activity is known as **drift**. The northern portion of the North American craton is covered in a sheet of glacial drift. Drift that has been transported by wind is a major component of **loess**, wind-blown silt and clay. Drift that has been processed by fluvial action becomes sorted by size and density, and is therefore known as **stratified drift**.

FIGURE 1 (*a*) The origin of an end moraine. (*b*) End moraines are described as terminal moraines or recessional moraines depending on their relative positions with respect to the glacier that produced them.

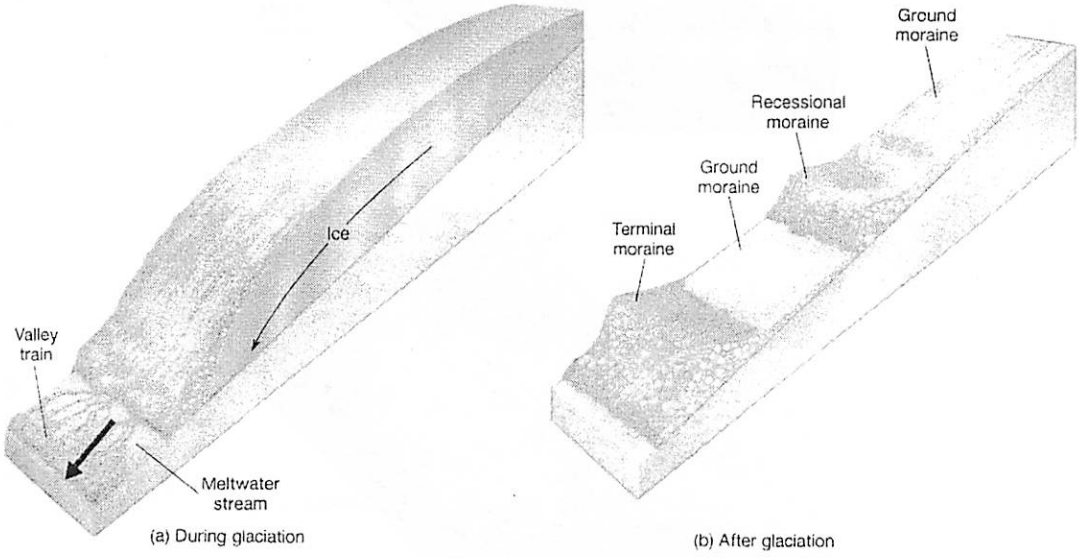

The sediment deposited directly by the glacial ice is **till**. Landforms composed of till are known as **moraines**. There are three major classes of moraines: end moraines, ground moraines, and lateral moraines. Fig.1 shows two of these (from Monroe and Wicander, 1992). **End moraines** form at the terminus of a glacier, especially when the glacier has a balanced ice budget for a few years. The end moraine at the greatest extent of the glacier is the **terminal moraine**. The terminal moraines in the White mountains have been subsequently worked by fluvial processes, and are not very visible. The geologic map of the White mountains (p. 10) shows a dashed line at the best guess for the location of the terminal moraine. **Recessional moraines** are much more common, occurring at any location where the ice front stabilized as it receded. Even among these, the oldest recessional moraines are much more pristine in the White mountains. Moraines from the Purcell and Smith Cienega glaciations are typically cut by subsequent stream beds. **Ground moraines** are composed of basal till that has been transported subglacially (see Fig. 4, from Fenn, 1987). **Lateral moraines** are formed along the margin of a glacier. When several lateral moraines merge, as when valley glaciers converge, they create **medial moraines**, running down the center of the glacier.

When a glacier has a stream running underneath it a sedimentary deposit known as an **esker** develops (see Fig. 2). Large boulders are sometimes transported by glaciers, these are known as **glacial erratics**.

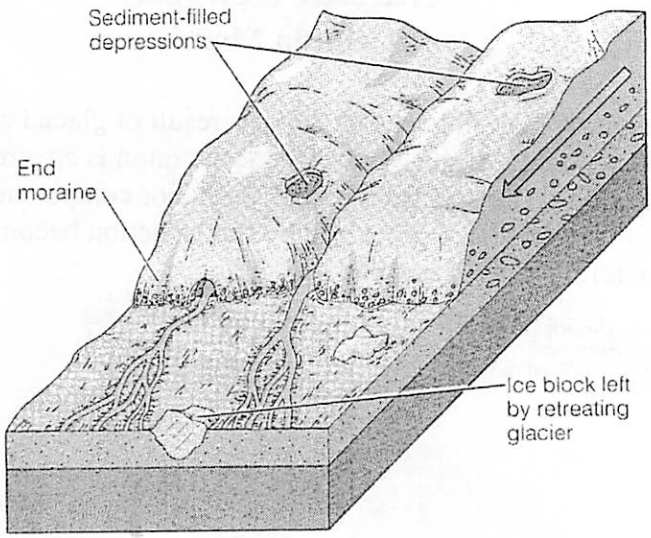

(a)

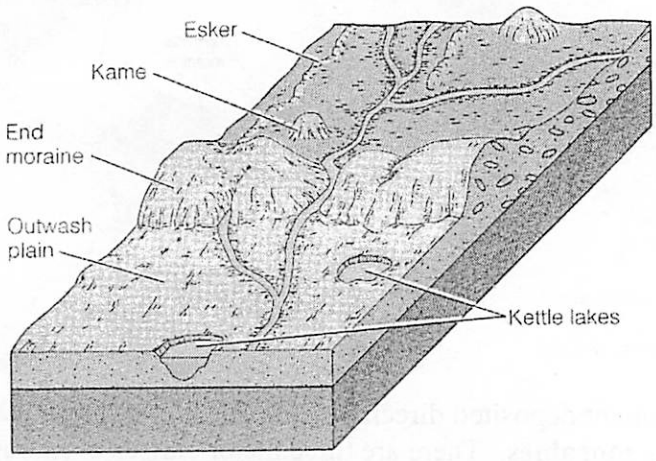

(b)

FIGURE 2 Two stages in the origin of kettles, kames, and eskers. (*a*) During glaciation. (*b*) After glaciation.

Glaciers are very effective at creating both depression and dams that lead to lakes forming downstream from them as they retreat. We will observe this phenomenon in the many cienegas along the lower flanks of the White Mountains. These lakes often collect sediment in distinctive patterns, due to the control on their sedimentation rates by the nearby glacier. Two common features are varves and dropstones, illustrated in Fig. 3. **Varves** are finely laminated, alternating light and dark layers deposited in an annual cycle. During the spring and summer when runoff from the glacier is at its height light layers of sand and clay are deposited. In the winter only the smallest of clays and organic matter settle down from the still and often frozen-over lake. **Dropstones** are gravel to boulder size objects that are rafted out to the lake interior on chunks of ice.

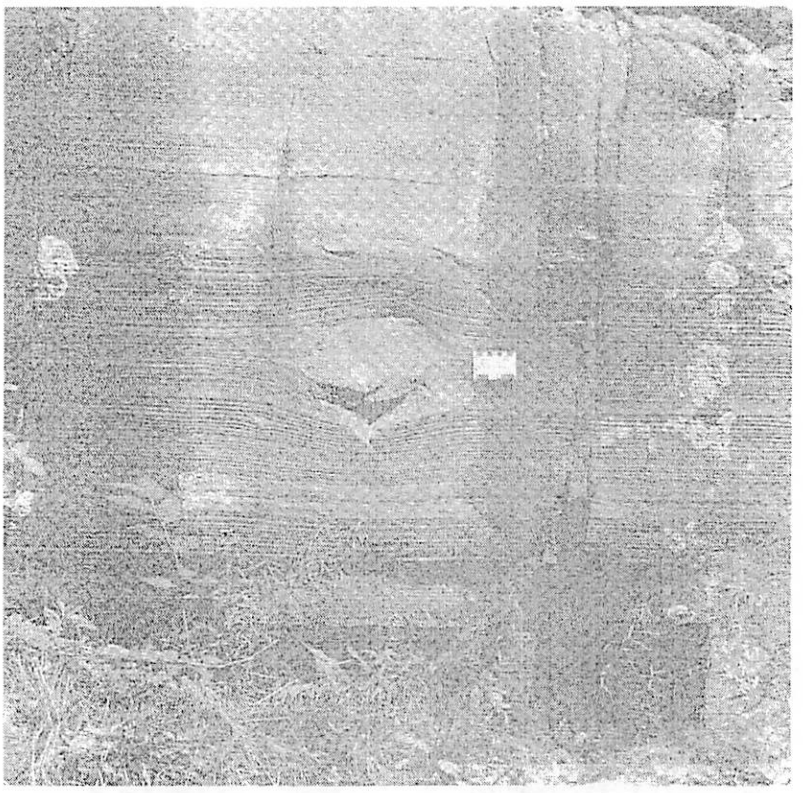

FIGURE 3 Glacial varves with a dropstone.

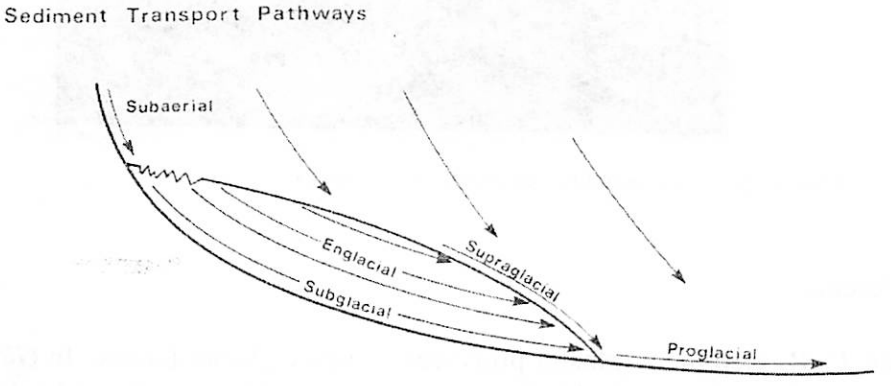

FIGURE 4

There are four transport paths for drift associated with glaciers. These are illustrated in Fig. 4 (Fenn, 1987). Subglacial transport forms eskers and ground moraines. Englacial transport is associated with lateral and medial moraines. An example of engalcial transport is provided in Fig. 5, (Fenn, 1987). Supraglacial transport on top of the glacier is a major contributor to end moraines. Proglacial processes form braided streams of drift material and the glacial lake deposits typified by varves and dropstones.

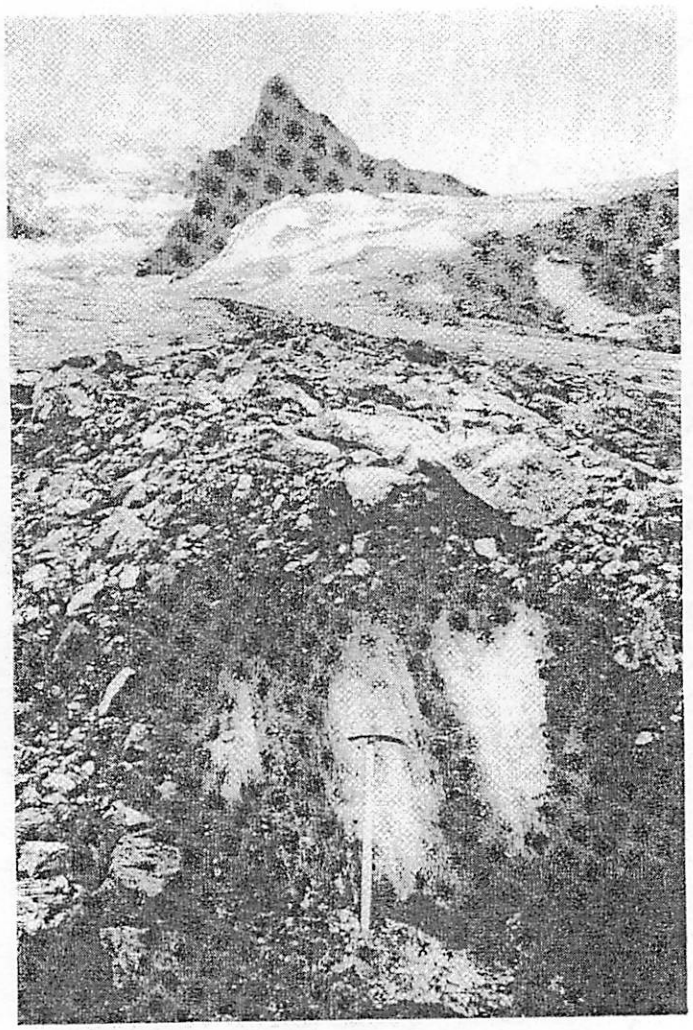

FIGURE 5 Longitudinal englacial debris bands

Reference:

Fenn, C. R., Sediment transfer processes in alpine glacier basins. In *Glacio-fluvial Sediment Transfer: An Alpine Perspective*. Eds. A. M. Gernell and M. J. Clark. Jowhn Wiley and Sons: New York, 1987.

Monroe, J.S. and R. Wicander. Physical Geology: Exploring the Earth. West Publishing Company: New York, 1992.

Glacial Geomorphology: Erosion

By
C.S. Cooper

1. Introduction

Glaciers form from successive annual layers of snow that accumulate and persist through the summer melting season. These layers of moderately compact snow having a bulk density of 0.5 to 0.8 g/cm^3 are called **firn** in German or **névé** in French. Both terms are widely used in English. As firn is compacted, individual ice grains freeze together, increasing the bulk density up to 0.8 to 0.9 g/cm^3, which is close to that of pure ice, which has a bulk density of 0.916 g/cm^3.

Glacial erosion is the process by which glaciers act as "geomorphic agents" that erode the rocky surfaces over which they travel, thereby transporting sediments across vast distances of land. An understanding of glacial geomorphology requires first an appreciation of the formation and flow of glacier ice. Depending on their thermal structure, the ice thickness, and type, glaciers can have a wide variety of erosional effects.

2. Plasticity of Ice

The key idea underlying our theoretical understanding the flow of glaciers is the plastic deformation of ice as a power law equation, called Glen's flow law:

$$\frac{d}{dt}\varepsilon = A\,\tau' \quad \text{(Equation 1).}$$

In Equation 1, the left hand side d/dt(ε) is the creep rate, τ is the shear stress, and A and n are constants. The exponent n is typically ~3. Hence, glacier flow rate goes as the third power of the shear stress, i.e., an order of magnitude increase in the shear stress represents *three* orders of magnitude increase in the glacial creep rate. The constant A in Equation 1 depends on the glide plane of the ice crystal lattice. Deformation along the "easy glide" plane is typically 500 times faster than deformation along the "hard glide" plane of the crystal.

3. Major Types of Glaciers

Cold, Polar, or Dry-base Glaciers – basal ice frozen firmly to underlying rock.
Temperate Glaciers – pressure depresses the melting point of ice slightly, resulting in a liquid phase between the rock and ice. Typically flow twice as fast as polar glaciers.
Intermediate Glaciers – intermediate between the two types of glaciers above having a very thin (~1 mm) liquid water phase between the rock and ice sheet.

4. Glacial Flow

- Ice can flow "uphill" over and around obstacles on its rock floor because the direction of the flow is controlled by the surface slop of the glacier, not the slope of the rock bed beneath it.
- Models taking ice to flow as a plastic with rheidity defined by Glen's flow law (Equation 1) works well but not perfectly.

- Solid state recrystallization results in reorientation of ice crystals during movement under shearing stresses.
- Basal slip is an important effect, in which local shear stresses increase near the base of a glacier where the rock protrudes up into the ice, greatly increasing the ice deformation. This **enhanced plastic flow** is proportional to the size of the obstruction.
- If ice is at or very close to the melting temperature, an additional type of basal movement is possible, known as **regelation slip**. This process involves temperature dependent freezing and melting, which is essentially an isothermal process.
- Mathematical models have not been successful in general in reproducing basal slip.

5. Erosion and Sedimentary Transport

- Processes and Bedforms
  Eroded rock masses produce *detritus* (loose rock) that is carried by the glacier. Unlike in aeolian and fluvial transport processes, glaciers transport all grain sizes, which are often thoroughly mixed within the ice.
- Glaciotectonism
  Effective stress applied to the rock substrate by the weight of overlying ice affect motion of rock beds.
- Crushing and Fracture
  Glacier ice itself cannot create pressures in excess of the crushing strength of rock. However, at a point contact between a rock particle embedded in the ice and the rock substrate, pressure is adequate to chip or flake both the particle and the substrate. Distinctive features on fractured rock include *chattermarks* and *crescentic fractures.*
- Plucking and Hydraulic Jacking
  Rock fragments can be incorporated into the regelation layer and carried away by the glacier, called *plucking*. A related process involves rapid increase of water pressure in sub-ice cavities that causes basal ice to move suddenly, pushing joint-bounded blocks of rock forward. The process is known as *hydraulic jacking*.
- Abrasion
  Rock fragments within ice cause the abraded scratches and groves characterizing glaciated rock, not the ice itself. Abrasional effectiveness depends on the relative hardness of the "tool" held by the ice and rock substrate.
- Fluvial Erosion Beneath Glaciers
  The basal film of water observed beneath temperate and intermediate glaciers is not capable of mechanical erosion, but it can chemically corrode carbonate rocks. However, in subglacial channels, the relatively warm and often muddy melt-water can erode the base of the ice and the bedrock or sediment beneath the ice. *Potholes* in bedrock eroded by vortices in subglacial rivers are well-known landforms. Also, *tunnel valleys* were eroded into unconsolidated sediments along some late Pleistocene ice sheets. This is also the source of almost all the outwash in front of the Malaspina Glacier in Alaska.

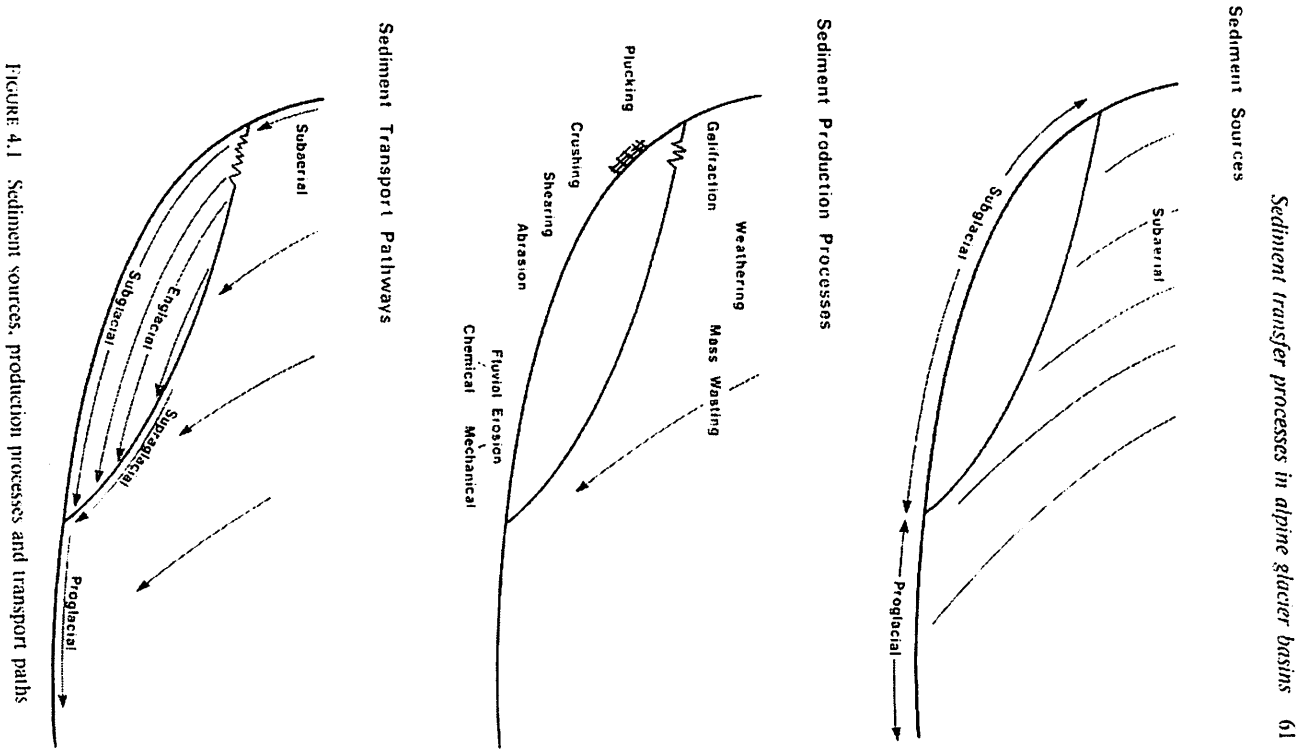

FIGURE 4.1 Sediment sources, production processes and transport paths

References

Bloom, Arthur L. *Geomorphology, 3rd Edition.* Upper Saddle River, New Jersey: Prentice Hall, 1998, 1991.

N.B. Because I did not have time to study other sources, my primary reference for this field trip handout and oral presentation ended up being this book, which I borrowed from Michael Bland's bookshelf (thanks!). The concepts described herein represent a terse summary of the major points of Bloom's discussion of glacier formation, flow, and glacial geomorphology as presented in Chapters 16 and 17 of the book. This book is excellent, and it of course contains much more detailed information on the subjects of glacial flow and glacial geomorphology as well as a detailed discussion of the related topic of periglacial geomorphology in Chapter 14.

Merrill, R.K. and Péwé, T.L., "Late Cenozoic Geology of the White Mountains, Arizona." *State of Arizona Bureau of Geology and Mineral Technology, Special Paper No. 1* (1977), Tucson: University of Arizona.

N.B. This reference presents more specific information on the geology of the White Mountains of Arizona.

Global Climate Over the Past Few Million Years

Carl W. Hergenrother
PTYS 594a
Fall 2003

Methods of Study

Numerous methods have been developed to study past climates. The methods analyze a number of varied chemical, physical and biological variables. The majority of methods involve the detection of material within core samples. Table 1 lists a number of different techniques, what they measure and what they tell us about past climates.

Characteristics of Some Paleoclimatic Data Sources

Proxy data source	Variable measured	Continuity of evidence	Potential geographic coverage	Period open to study (year B.P.)	Minimum sampling interval (year)	Usual dating accuracy (year)	Climatic inference
Layered ice cores	Oxygen isotope concentration, thickness (short cores)	Continuous	Antarctica, Greenland	10,000	1–10	±1–100	Temperature, accumulation
	Oxygen isotope concentration (long cores)	Continuous	Antarctica, Greenland	100,000+	Variable	Variable	Temperature
Tree rings	Ring-width anomaly, density, isotopic composition	Continuous	Midlatitude and high-latitude continents	1,000 (common) 8,000 (rare)	1	±1	Temperature, runoff, precipitation, soil moisture
Fossil pollen	Pollen-type concentration (varved core)	Continuous	Midlatitude continents	12,000	1–10	±10	Temperature, precipitation, soil moisture
	Pollen-type concentration (normal core)	Continuous	50° S to 70° N	12,000 (common) 200,000 (rare)	200	±5%	Temperature, precipitation, soil moisture
Mountain glaciers	Terminal positions	Episodic	45° S to 70° N	40,000	—	±5%	Extent of mountain glaciers
Ice sheets	Terminal positions	Episodic	Midlatitude to high latitudes	25,000 (common) 1,000,000 (rare)	—	Variable	Area of ice sheets
Ancient soils	Soil type	Episodic	Lower and midlatitudes	1,000,000	200	±5%	Temperature, precipitation, drainage
Closed-basin lakes	Lake level	Episodic	Midlatitudes	50,000	1–100 (variable)	±5% ±1%	Evaporation, runoff, precipitation, temperature
Lake sediments	Varve thickness	Continuous	Midlatitudes	5,000	1	±5%	Temperature, precipitation
Ocean sediments (common deep-sea cores, 2–5 cm/1000 years)	Ash and sand accumulation rates	Continuous	Global ocean (outside red clay areas)	200,000	500+		Wind direction
	Fossil plankton composition	Continuous	Global ocean (outside red clay areas)	200,000	500+	±5%	Sea-surface temperature, surface salinity, sea ice extent
	Isotopic composition of planktonic fossils; benthic fossils; mineralogic composition	Continuous	Global ocean (above $CaCO_3$ compensation level)	200,000	500+	±5%	Surface temperature, global ice volume; bottom temperature and bottom water flux; bottom water chemistry
(rare cores, >10 cm/1000 years)	As above	Continuous	Along continental margins	10,000+	20	±5%	As above
(cores, <2 cm/1000 years)	As above	Continuous	Global ocean	1,000,000+	1000+	±5%	As above
Marine shorelines	Coastal features, reef growth	Episodic	Stable coasts, oceanic islands	400,000	—	±5%	Sea level, ice volume

Table 1- List of different climate reconstruction tecniques. (From Hartmann 1994).

Causes of Climate Change

The Earth's climate is affected by many different driving forces, most of which are interconnected. Some of the more important drivers are as follows:

- variation in solar insolation due to changes in the Sun's energy output
- changes in the Earth's orbital parameters
    - 100,000 and 400,000 year period in the variation of eccentricity, or the ellipticity of the Earth's orbit
    - 40,000 year period in the variation of obliquity, or the tilt of the Earth's poles with respect to the Sun
    - 20,000 year period in the variation of the longitude of perihelion, or the location in the Earth's orbit of the perihelion point
- changes in the strength and direction of the prevailing winds due to the contraction and expansion of the circumpolar vortex
- volcanic eruptions and expulsion of dust and gases into the upper atmosphere
- long term changes in the abundance of greenhouse gases
- changes in ocean circulation patterns
- changes in continental positions

Climate from 1 million BP to 150,000 BP

During the course of the Earth's history, the climate has been predominately warmer than at present. A maximum in temperature occurred during the middle Cretaceous around 100 million year ago. Studies of ancient soils suggest that the atmospheric abundance of CO_2 was 4 to 6 times higher than at present. This may have been due to increased levels of volcanism during this period. Since the Cretaceous, the climate has become progressively colder. The main drivers for this cooling seem to be a decrease in atmospheric CO_2 and the movement of the continents away from Antarctica and the southern polar regions. The gradual cooling lead to development of ice sheets on Antarctica about 14 million years ago. By 5 million year ago, the volume of ice over Antarctica had reached its present value. In the northern hemisphere, the first appearance of ice occurred 3 million years ago.

The Quaternary ice age of the past few million years has been punctuated by periods of glacial advancement and retreat. Prior to 700,000 years before present (BP), the glacial-interglacial cycles had a rough period of 41,000 years. More recent than 700,000 years, the glacial-interglacial cycles had a longer period of 100,000 years and had become more extreme. Ice core measurements of the $^{18}O/^{16}O$ ratio ($\delta^{18}O$) reveal the extent of the climatic variations over the last 2.5 million years (Fig. 1). The gradual cooling over this time period and change in periodicity of the glacial-interglacial cycle 700,000 years ago is evident. The frequency spectrum of $\delta^{18}O$ variance show variations with periods around 23, 41, 96 and 480 thousand years (Fig. 2). The periods in $\delta^{18}O$ variance match up well with the variations due to changes in the Earth's orbital parameters. The longitude of perihelion cycle matches the 23,000 year variance cycle, the obliquity cycle matches the 41,000 year cycle, the 96,000 year variance cycle matches one of the eccentricity cycles while the 480,000 year variance cycle is a less perfect fit to the longer 600,000 year eccentricity cycle.

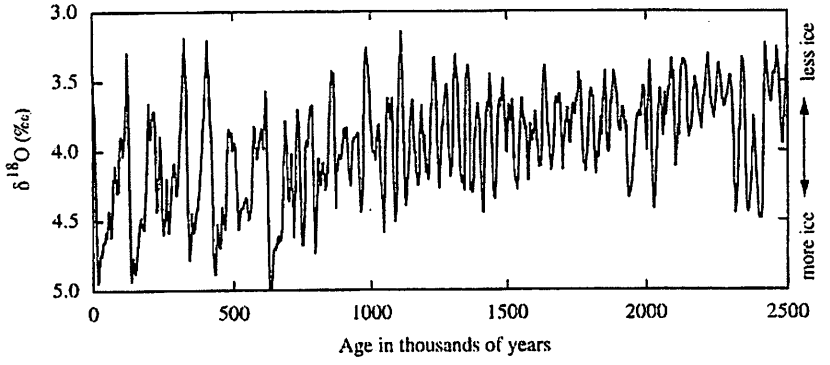

Fig 1 - $\delta^{18}O$ values over the past 2.5 million years (from Hartmann 1994).

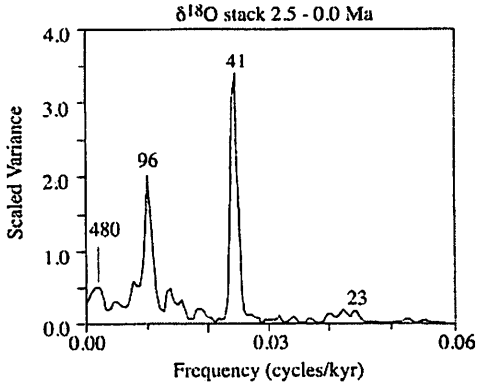

Fig. 2 - Frequency spectrum of $\delta^{18}O$ variance (from Hartmann 1994)

Climate from 150,000 BP to Present

The past 150,000 years has seen the climate swing from a warm interglacial period to the depths of a cold glacial maximum and back again. Around 130,000 to 110,000 years BP, the Earth's climate was very similar to today. This is referred to as the Eemian interglacial (point 5 in Fig. 3). During this period, there

is ice core and pollen analysis evidence of sudden and short-lived downturns in temperature and precipitation (strong event ~120,000 years ago). Suddenly around 110,000 years BP, the climate reentered a glacial period. High resolution sediment records from the Atlantic suggest that the transformation to cold glacial conditions may have taken place in *only* 400 years (Adkins et al. 1997). The globe continued to cool until 70,000 years BP. For the next 40,000 years, conditions warmed though it was still much colder than present. Around 30,000 years BP, conditions worsened once again. Ice sheets reached their greatest extent between 21,000 and 18,000 years BP. During these cold conditions the aridity of the globe reaches a maximum as the amount of water evaporating from the oceans and precipitating on the continents is at a minimum. This is due to the drop in mean sea surface temperature which ranges from 0 to 14 degrees Celsius lower than present.

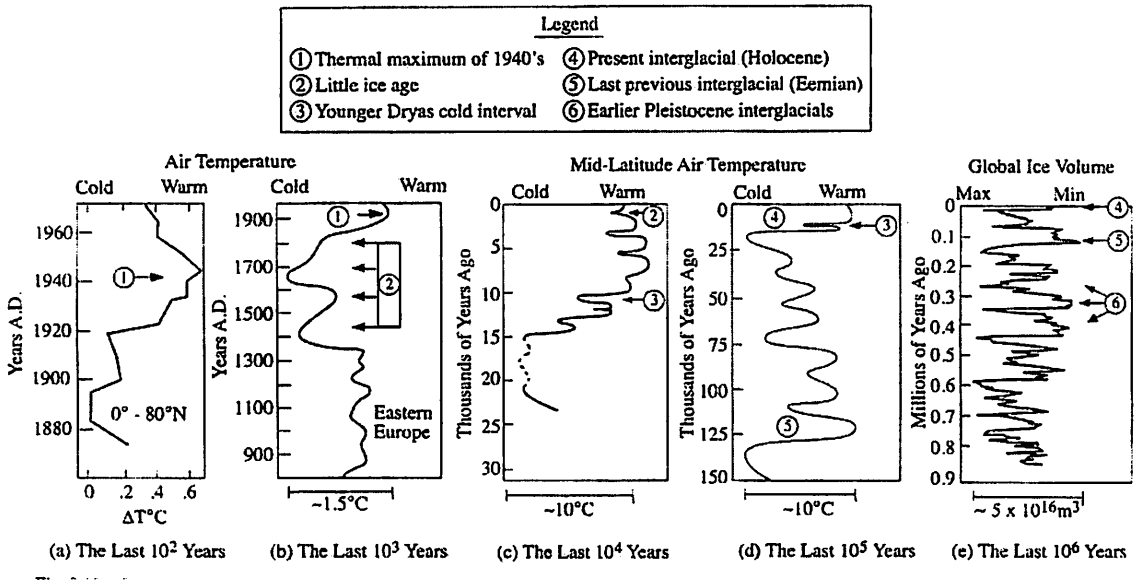

Fig. 3 - Temperature tends over tha past million years (from Hartmann 1994).

Beginning around 14,000 years BP, the climate rapidly began to warm. The ice sheets retreated, forests expanded and the world became wetter. By 13,500 years BP, most of the world was at least as warm as today. A short reversal in the warming trend occurred around 12,000 years BP (point 3 in Fig. 3). This episode, called the 'Younger Dryas', was constrained to the northern Atlantic region and may not have greatly affected the Arizona region. The cool spell may have been the result of the shutdown of the deep thermohaline circulation of the North Atlantic due to the melting of the North American Laurentide ice sheet and the release of large quantities of fresh water into the North Atlantic. The climate reached its warmest between 9000 and 5000 years BP.

A general timeline covering the past 150,000 years from the 'Global land environments since the last interglacial" webpage at http://members.cox.net/quaternary is included below.

150,000 y.a. - cold, dry full glacial world

130,000 y.a. - rapid warming initiates the Eemian interglacial

130,000-110,000 y.a. - global climate generally warmer and moister than present, but with progressive cooling to temperatures more similar to present.

121,000 y.a. - possible global cold, dry event

?110,000 y.a. - a strong cooling marks the end of the Eemian interglacial

105,000-95,000 y.a. - climate warms slightly but still cooler and drier than present; strong fluctuations.

95,000 - 93,000 y.a. - another cooler phase similar to that at 110,000 y.a.

93,000 - 75,000 y.a. - a milder phase, resembling that at 105,000-95,000 y.a.

75,000 - 60,000 y.a. - full glacial world, cold and dry (the 'Lower Pleniglacial')

60,000 - 25,000 y.a. - 'middling phase' of highly unstable but generally cooler and drier-than-present

25,000 - 15,000 y.a. - full glacial world, cold and dry; Stage 2 (includes the 'Last Glacial Maximum')

14,500 y.a. - rapid warming and moistening of climates in some areas. Rapid deglaciation

13,500 y.a. - nearly all areas with climates at least as warm and moist as today's

12,800 y.a. - rapid onset of cool, dry Younger Dryas in many areas

11,500 y.a. - Younger Dryas ends suddenly, back to warmth and moist climates

9,000 - 8,200 y.a. - climates warmer and often moister than today's

~ 8,200 y.a. - sudden cool and dry phase in many areas

8,000 - 4,500 y.a. - climates somewhat warmer and moister than today's

Since 4,500 y.a. - climates fairly similar to the present

References

The information in this handout was collected from the following paper and three books.

Adkins, J.F., Boyle, E.A., Keigwin, L. & Cortijo, E. (1997). Variability of the North Atlantic thermohaline circulation during the last interglacial period. *Nature* **390**, p.154-156.

Hartmann, D.L. (1994). Global Physical Climatology. Academic Press, San Diego.

Lamb, H.H. (1982). Climate History and the Modern World. Metheun & Co. Ltd., New York.

Sellers, W.D. (1965). Physical Climatology. The University of Chicago Press, Chicago.

Mommy – Where is the Sky Blue?

Jason W. Barnes
Department of Planetary Sciences, University of Arizona, Tucson, AZ, 85721
jbarnes@c3po.barnesos.net

ABSTRACT

In our solar system, when standing on a solid surface, the sky is blue on only the Earth. Mars' sky is pink due to dust scattering, and rayleigh scattering is unimportant. For planets with thicker atospheres than we have, there should be a point in the upper atmosphere where the sky looks blue, provided there aren't any clouds or dust obscuring the view.

Subject headings:

WHY IS THE SKY BLUE?

To answer the question "where is the sky blue?", first we'll start with that old, pedestrian question, "why is the sky blue?".

Earth's sky is blue due to *Rayleigh Scattering*. Light, electromagnetic radiation, is a travelling wave of alternating electric and magnetic fields. When a plane wave of light from say, the Sun, is incident upon atoms and molecules in an atmosphere, the wave passes through the individual electric and magnetic fields of the atomic protons and electrons. These atomic electromagnetic fields disrupt the plane wave by an amount depending on light's wavelength, with smaller wavelength light being disrupted more – the disruption is similar to the atmospheric scattering of light through isoplanatic patches that are the cause of telescopic seeing. The scattering phase function is nearly isotropic, though, due to the small size of the disruptions to the wave (see Boehm-Vitense (1989) Volume 2 p 81 for Fortney's preferred alternative quantum mechanical explanation).

The fraction of light scattered depends on the Rayleigh scattering cross section σ_R (Hubbard et al. 2001):

$$\sigma_R = \frac{8\pi^3(2+\nu)^2\nu^2}{3\lambda^4 N^2}, \quad (1)$$

where ν is the refractivity (refractive index minus 1.0), N is the number density of the molecules in question, and λ is the wavelength. Our sky is blue because of this λ^{-4} dependence – blue light is scattered much more easily than red light. I've included some refractivities for relevant potential atmospheric constituents (from Cox (2000)) in Table 1

STRUCTURE OF A BLUE SKY

The thing to notice about Table 1 is that oxygen, nitrogen, carbon dioxide, water vapor, and even hydrogen aren't all THAT different in their refractivity, and therefore in their rayleigh scattering cross-section. Okay, so they vary by an order of magnitude or so in $(2+\nu)^2$ – bah. Its only ONE order of magnitude! In the end, with some generous approximations, you can do good rough figuring in your head. The bottom line is that the most important factor affecting Rayleigh scattering is the column abundance of gas in the path in question (Figure 1). If that quantity is roughly the same as that on Earth's surface, the sky looks blue, otherwise it doesn't. Of course, that's assuming you're on Earth looking straight up, where there is the lowest column abundance of gas molecules. The column abundance (in a plane-parallel approximation) goes as $1/\cos(\text{zenithdistance})$ (see Figure ??), a quantity that astronomers refer to as an 'atmosphere' (i.e., "wow, you're over at 3.5 atmospheres, the seeing has to be shit!").

Earth's atmospheric scale height is 8km, about the height 737's fly across the US. There's 1/3 the pressure there, and so to zeroth order there's 1/3 the column abundance and rayleigh scattering is 1/3 as important. I seem to remember that when I'm on a plane the sky is a darker blue from up there, but I might just be making that up for convenience at the moment. I'll have to look next time. Air Force pilots are given astronaut's wings (kind of an oxymoron, really) at 100,000 ft, about 3 scale heights or 1/30th the column abundance at the surface. Supposedly the sky is pretty damned black up there, perhaps a dark indigo.

BLUE SKIES IN THE SOLAR SYSTEM

Lets apply this to other planets. Mars' surface pressure is 0.006 bars. Its gravity is 1/3 that of Earth, though, so the scale height is higher, and the column abundance (love those cm-Am!) is 3 times 0.006: still pretty small at 0.018. Since Mars' column abundance of gas molecules is only 1.8% that of Earth's, Rayleigh scattering is relatively unimportant in the optical. By this calculation, the sky on Mars should be black, maybe dark purple. However, images clearly show Mars' sky to be pink! (see Figure 3) This turns out to be the result of multiple backscattering off of individual suspended dust particles in Mars' lower

TABLE 1
REFRACTIVITIES OF SELECTED GAS SPECIES

Gas	Refractivity (n-1)
H_2	1.384×10^{-6}
He	0.350×10^{-6}
O_2	2.72×10^{-6}
N_2	2.97×10^{-6}
(air)	2.918×10^{-6}
H_2O	2.54×10^{-6}
CO_2	4.498×10^{-6}
CH_4	4.41×10^{-6}

NOTE.—Refractivities (ν) are determined at standard temperature and pressure.

Fig. 1.— This is a fateful image. The older, hackneyed folks will see Fred and Dave, dancing on the top of their vehicle to "I Like Big Butts" in the middle of Death Valley. The younger, bushy-tailed fieldtrippers (are there any on this trip?) will note that although the shadows of the foreground hills and background mountains are of equal intrinsic brightness, the mountains appear with higher brightness and lower contrast due to rayleigh scattering of sky-blue light into the beam in the 20 or so miles between us and those mountains. (photo from Ross Beyer)

Fig. 2.— View of the Earth's atmosphere that I took from the east coast of Baja California looking out over the Gulf of California. Note the increase in saturation (as in hue, saturation, value) as a function of zenith distance.

atmosphere.

Okay, now move to a Blue Mars scenario, with Mars happily terraformed to have 1 bar of 78% nitrogen and 22% oxygen, with its current 0.6% carbon dioxide left as-is. This Kim-Stanley-Robinsonesque wonderland has 3 times Earth's column abundance due to the gravity/scale height effect, and so its sky isn't blue! At least, not as blue as Earth's. It should instead look pretty white, as white as Earth's atmosphere 20° above the horizon. So, when terraforming Mars, try to go with 0.22 bars partial pressure of oxygen, but cut back on the nitrogen to like 0.11 bars, okay? You won't need any more than that; the martians can just follow the high-altitude directions on their pot-pies.

Venus' surface is right out. There's 90 bars above you (and 90 times Earth's column abundance), and besides its all scattered by clouds (Figure 5). The sky is surprisingly bright, though, and supposedly slightly reddened by cloud absorption. But how about above the clouds? What if VISE has an imager, would it see blue sky above the clouds? Venus' cloud tops are at like 60km altitude, and its scale height is 16 km near the surface (its lots hotter than Earth). At 3 scale heights then it there should only be 3 times Earth's column abundance above you: the sky would be a very light blue. Go up another scale height (to like, say, 75km or so) and it might very well be an Earth-like blue!

Titan is a real pain in the ass to do in your head like this, just because its radius and gravity are small enough that curvature is important, gravity isn't constant over the atmosphere, and that kind of stuff. However, there should exist a point in Titan's atmosphere where the column abundance above you would be about the same as Earth's, and in which the sky should appear blue. Prediction of this effect is attributed to early space artist Chelsey Bonestell, who painted pictures from Titan's surface with a blue sky. Totally pre-Voyager. It would be a competition between rayleigh scattering and haze, and I won't hazard a guess as to which would win, though others have. They claim that in Titan's stratosphere the sky would look blue, and they call it the bonestellosphere in the artist's honor (Figure 6).

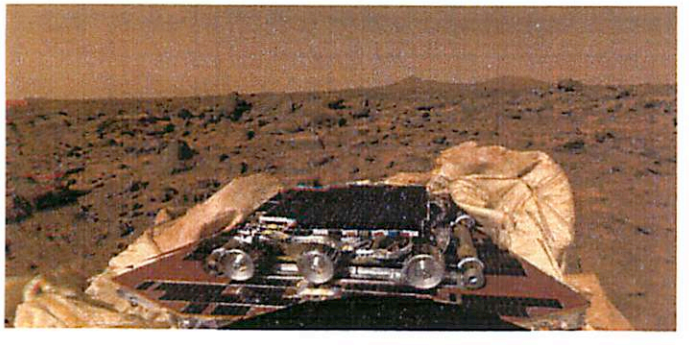

Fig. 3.— The sky on Mars, from IMP on Pathfinder. Left to Rayleigh Scattering alone, the sky would be black – the pink hue comes from multiple backscattering off of suspended dust particles.

To do this for real, you'd have to explicitly calculate the column abundance for each gas species using some sort of atmospheric model or data, and then add the total cross-sections together and compare it to Earth's. You could also do a full-up radiative transfer calculation, or a Monte-Carlo model (steer clear of a Las Vegas model, lest you be mauled by a white siberian tiger), but I don't think you'd necessarily get a much better big-picture idea of what's going on.

See `http://atmos.nmsu.edu/education_and_outreach/e` for an interesting look at the rayleigh scattering.

REFERENCES

Boehm-Vitense, E. 1989, Introduction to stellar astrophysics. Volume 1 - Basic stellar observations and data. Volume 2 - Stellar atmospheres (Cambridge and New York, Cambridge University Press, 1989, 251 p.)

Cox, A. N. 2000, Allen's astrophysical quantities (Allen's astrophysical quantities, 4th ed. Publisher: New York: AIP Press; Springer, 2000. Editedy by Arthur N. Cox. ISBN: 0387987460)

Hubbard, W. B., Fortney, J. J., Lunine, J. I., Burrows, A., Sudarsky, D., & Pinto, P. 2001, ApJ, 560, 413

This 2-column preprint was prepared with the AAS LaTeX macros v5.0.

Fig. 4.— Sunset on Mars, from Viking.

Fig. 5.— The surface and sky of Venus, from the Venera 13 lander. Surface lighting is always diffuse, as it is always overcast. Think of sitting in your oven while its on the 'self clean' cycle while in Seattle.

Fig. 6.— Painting by Kim Poor of Titan's Bonestellosphere.

The Geology and Stratigraphy of the Colorado Plateau and Canyon de Chelly

Tamara Goldin
Lunar and Planetary Laboratory and Department of Geosciences, University of Arizona, AZ 85721

Introduction

Simply stated, the Colorado Plateau is a broad expanse of high country dotted by high mesas, pinnacles, smaller plateaus, deep canyons, and laccolith mountain ranges (Baars 2002). It is a semi-arid desert with average elevations of 5000 feet.

The exact boundaries of the Colorado Plateau are not well established. Mountainous regions surround the plateau, but transitions to flat-lying land are gradual and interpretations vary as to where the boundaries lie. It has been proposed that major fracture zones in the Precambrian basement rock control the location and orientation of the major geologic features, including the boundaries of the plateau (Baars 1983, Baars 2002, Fig. 1). These fault zones, containing complex swarms of wrench faults where the movement of fault blocks is mainly strike-slip, have been active since 1.6-1.7 billion years ago (Baars 2002). The pattern of the basement wrench fault zones is of northwest-southeast-directed faulting and northeast-southwest-oriented fault zones.

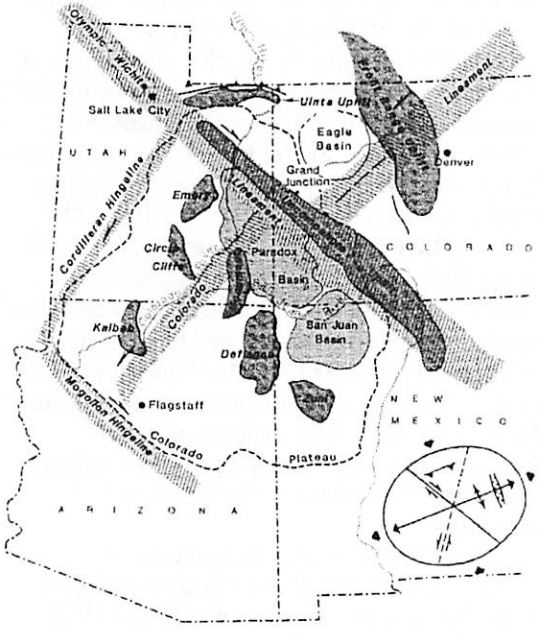

Figure 1. The Colorado Plateau and its major fault zones. Major geologic uplifts are shaded. From Baars 2002.

Geology of the Colorado Plateau

The surface geology of the plateau is marked by monoclinal folds, generally oriented north-south, and their associated uplifts. The faults underlying the draping sedimentary rocks are formed by west-east crustal extension and the steep sides of the monoclines mostly face east (Baars 2002). One of these monoclinal uplifts is the Defiance Uplift, which contains Canyon de Chelly. Between such uplifts are basins, which became major depositional structures with the uplift and rapid erosion during the Laramide Orogeny (75-50 Ma). The Defiance Uplift is bordered by the Black Mesa Basin to the west and the San Juan Basin to the east (Fig. 2).

Stratigraphy of the Colorado Plateau

A general geologic time scale and associated formations is shown in Table 1. In the Grand Canyon region, metamorphic Precambrian rocks are overlain by Paleozoic sedimentary units and are capped by the Permian Kaibab limestone. Of interest to us at Canyon de Chelly is the Permian sequence of red beds. The red sediments were likely deposited in continental environments (e.g. flood plains, lakes, dunes, deltas) in oxidizing conditions thus producing a hematitic cement between grains. The middle Permian is punctuated by two marine transgressions, which deposited the marine limestones and shales of the Toroweap and Kaibab formations (Baars 1983).

Mesozoic stratigraphy is absent at the Grand Canyon, but is exposed elsewhere on the plateau. In the late Permian the seas withdrew to the west and the Triassic is dominated by continental conditions and resulting red strata of mostly fluvial origins (Baars 1983). Mesozoic rocks are found surrounding the major uplifts, such as the Defiance, because the soft sedimentary strata are easily eroded from the crests of the uplifts, which formed in the Late Cretaceous and early Tertiary.

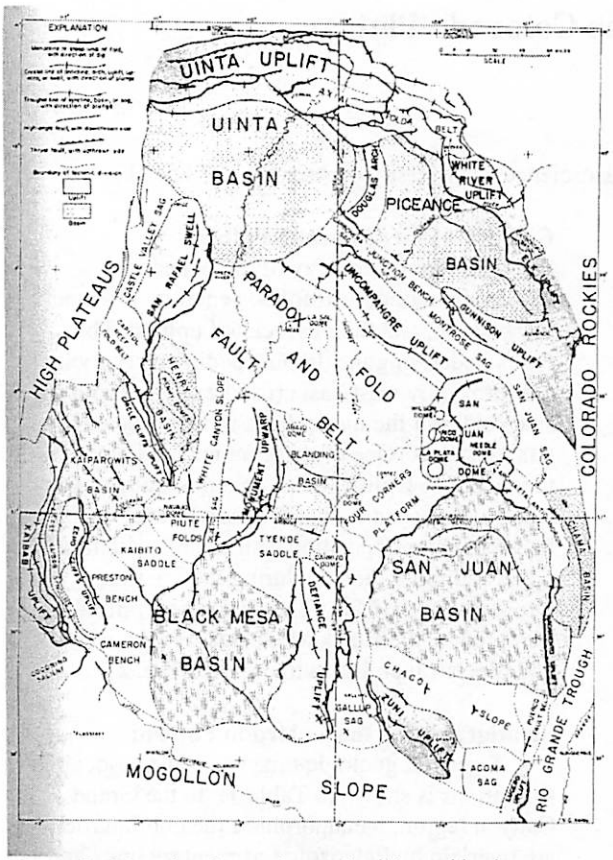

Figure 2. Map showing regions of uplifts and basins in the Colorado Plateau province. Faults are also marked. From Baars 1987.

Geology of Canyon de Chelly

From 350 A.D. to 1300 A.D. the Anasazi inhabited Canyon de Chelly and were followed in 1700 by the Navajo (Murray 1998), but the history of these red is much older. The red-orange cliffs, most dramatic in the Inner Canyon around the White House Ruins (Murray 1998) are composed of De Chelly sandstone, a Permian formation named after this canyon. At the base of the canyon is the meandering Chinle stream, which originates in the Chuska Mountains to the east and terminates in the Chinle wash to the west.

Canyon de Chelly has been eroded from the western flank of the Defiance Plateau, which is the present-day expression of the Defiance Uplift (Baars 2002). This north-south anticline is actually a composite structure composed of individual northwesterly trending folds. It is a structural fabric localized by the underlying system of Precambrian fault zones, like many of the geologic structures on the Colorado Plateau.

All sedimentary layers of pre-Permian age thin along the uplift's flanks, suggesting that the Defiance Uplift has been a highland since the beginning of Paleozoic time. At the crest of the structure, near Fort Defiance, Permian rocks lie directly on Precambrian metamorphics (Baars 2002).

The canyon was formed by the erosional down cutting of Chinle Creek. Presently, the canyon is no longer being deepened, but is instead choked with sand from seasonal flooding (Baars 2002). This suggests the canyon was carved during wetter inter-glacial episodes when melt waters had greater erosive power (Baars 2002).

Stratigraphy of Canyon de Chelly

The oldest rocks found on the Defiance Uplift and in Canyon de Chelly are red mudstones and siltstones of early Permian age. These fine-grained sediments were deposited on continental lowlands and intertidal mudflats. These strata outcrop only at the base of Spider Rock at the confluence of Monument Canyon (Baars 2002). These rocks are labeled the Organ Rock Shale, which is a formation in the Cutler Group.

The massive pink sandstone, which forms the cliffs at Canyon de Chelly, is the De Chelly sandstone and is a formation also included in the middle Permian Cutler Group. It is thought to have formed on the coastal lowlands of the central Colorado Plateau (Baars 1983). This formation of fossil sand dunes is found in parts of Arizona, New Mexico, and Utah, but reaches a maximum thickness near Canyon de Chelly (Baars 1983). Spider rock is the only locality in the canyon where the entire section of De Chelly sandstone (~825 feet) is exposed (Baars 2002). ***On a side note, Spider Rock is the legendary home of the Navajo Spider Woman who taught the Navajos how to weave (Murray 1998).***

The De Chelly sandstone reflects the shape of the Defiance Uplift in Permian time (Baars 2002). East from Spider Rock, at the crest of the uplift, the sandstone has thinned to 200 feet. The thickest deposits (1000+ feet) of sandstone occur in Black Mesa basin to the west and the San Juan Basin to the east. This indicates that the Defiance Uplift was a high topographic feature during the time of De Chelly sandstone deposition.

The De Chelly sandstone consists of massive wedge-shaped cross-bedded packages with steeply inclined cross-strata (Baars 1983, Baars 2002, Fig. 3). The sands were deposited in an Aeolian environment and cross-beds represent bedding surfaces on the leeward side of dunes that wandered across the dry plains. The

prevailing wind direction was from the north and northeast, suggesting the de Chelly sands were derived from the Uncompahgre uplift (Baars 1983). Cross-bed sets are large (10-50 feet thick) indicating mature large dunes (Baars 2002).

No late Permian rocks are seen on the Defiance Uplift and instead the Late Triassic Chinle Formation, the Shinarump Conglomerate Member, lies directly atop the De Chelly Sandstone (Baars 2002). These are the irregular beds of dark brown conglomeratic sandstone seen at the rims of canyons and form the harder cap, protecting the softer underlying sandstone from erosion. The roads and viewpoints in Canyon de Chelly are built atop this formation. The scoured contact between the De Chelly Sandstone and the Shinarump beds is an erosional surface (unconformity) on which fluvial sand and gravel was deposited.

The Shinarump Member displays smaller cross-beds at flatter inclinations (Baars 2002). These are lens shaped rather than planar representing sand-filled fluvial channels (Fig. 3). Also, unlike the mature De Chelly Sandstone, the Shinarump is composed of course poorly-sorted sand and gravel-sized grains.

The remainder of the Triassic is seen in several other sedimentary members of the Chinle Formation, although these colored shale beds are seen only as erosional remnants in Canyon de Chelly. They are better seen west and south of the Defiance Uplift, constituting the "Painted Desert." No rocks of Jurassic age are seen at Canyon de Chelly, but there is evidence of Tertiary explosive volcanism (mostly ash deposits) seen on parts of the Defiance Uplift (Baars 2002).

References

Baars, D.L. (1983). *The Colorado Plateau: A Geologic History.* University of New Mexico Press, Albuquerque, 279 p.

Baars, D.L. (2002). *A Traveler's Guide to the Geology of the Colorado Plateau.* The University of Utah Press, Salt Lake City, 294 p.

Murray, J.A. (1998). *The Colorado Plateau.* Northland Publishing, Flagstaff, 278 p.

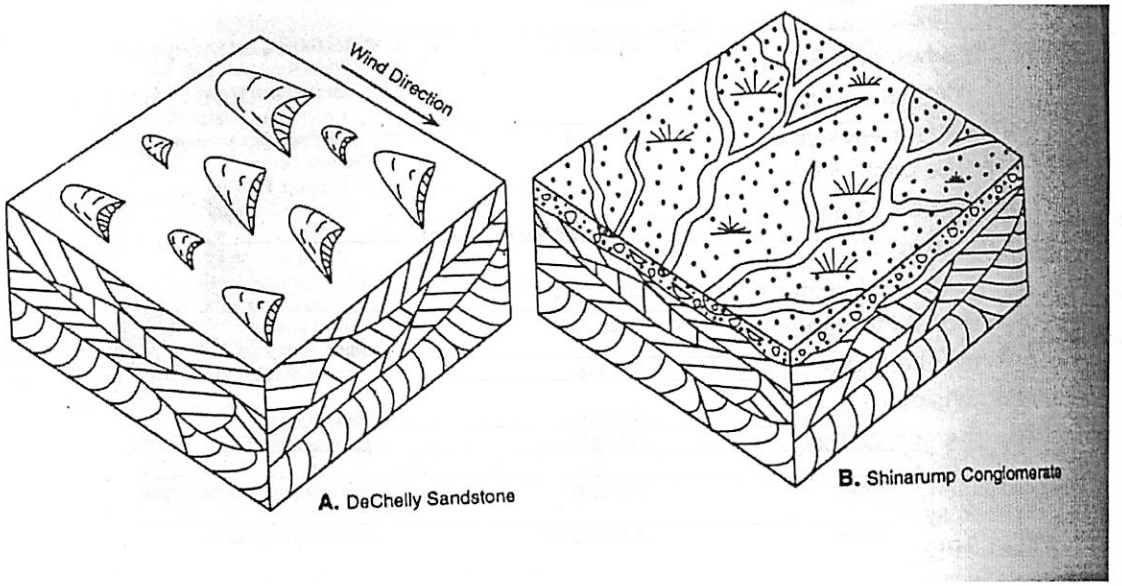

Figure 3. Cross-Bedding at Canyon de Chelly. A. Sand dunes drifting across the desert floor in Permian times formed high-angle cross beds seen in the De Chelly Sandstone. B. Meandering streams eroded the upper surface of the De Chelly sandstone in Late Triassic time, depositing the Shinarump Member consisting of lenticular beds of sand and pebbles with smaller, shallowly-dipping cross beds. From Baars 2002.

GEOLOGIC TIME SCALE

ERA	*PERIOD*	*MILLIONS OF YEARS AGO*	*FOUR CORNERS FORMATIONS*
CENOZOIC	Quaternary	0-1.6	soil, sand, gravel, terrace gravels
	Tertiary	1.6-65	Diatremes
			Igneous intrusives
			Chuska Formation
			Animas Formation/
			San Jose Formation
			Nacimiento Formation
MESOZOIC	Cretaceous	65-141	McDermott Formation
			Kirtland Shale
			Fruitland Formation
			Pictured Cliffs Sandstone
			Lewis Shale
			Mesaverde Group
			Cliff House Sandstone
			Menefee Formation
			Point Lookout Sandstone
			Mancos Shale
			Dakota Sandstone
			Cedar Mtn./Burro Canyon Formation
	Jurassic	141-208	Morrison Formation
			Summerville/Wanakah
			Entrada Sandstone
			Carmel Formation
			Navajo Sandstone
			Kayenta Formation
			Moenave/Wingate Ss.
	Triassic	208-245	Chinle Formation
			Moenkopi Formation
PALEOZOIC	Permian	245-290	Cutler Group:
			White Rim/ DeChelly Ss.
			Organ Rock Shale
			Cedar Mesa Sandstone
	Pennsylvanian	290-322.8	Elephant Canyon/Halgaito Fm.
			Hermosa Group:
			Honaker Trail Fm.
			Paradox Formation
		(Rocks below not exposed)	
			Pinkerton Trail Fm.
			Molas Formation
	Mississippian	322.8-362.5	Leadville/Redwall Fm.
	Devonian	362.5-408	Ouray Limestone
			Elbert Formation
	Silurian	408-438	Rocks missing
	Ordovician	438-510	Rocks missing
	Cambrian	510-570	Ignacio-Lynch Fms.
PRECAMBRIAN	Upper	570-2,500	Quartzite/granite/metamorphic
	Lower	2,500-4,500?	Metamorphic/granite

Table 1. Geologic timescale and stratigraphy of the Colorado Plateau province.

Groundwater Sapping Features on the Colorado Plateau

Jim Richardson

What is Groundwater Sapping?

Groundwater sapping is an erosional mechanism which forms entrenched, theater-headed canyon systems in some areas of the Colorado Plateau. It results from the undermining and collapse of valley head and canyon side walls by weakening or removal of basal support as a result of enhanced weathering and erosion by concentrated groundwater outflow at a site of seepage. (quoted from J. Laity).

Requirements for Groundwater Sapping

For groundwater sapping to occur, a rather constraining set of requirements must be met. These include (See *Figure 1*):

(1) **A permeable aquifer**. On the Colorado Plateau, massive sandstones form the aquifer layers, having high porosities (20-35%), high permeabilities (0.02-1.00 darcy), and extensive fractures and jointing due to exfoliation (stress-relief fractures from to the removal of overburden pressure). Rainfall penetration into these sandstones is empirically 0.5-3 inches within 20 minutes after the beginning of surface wetting. The Navajo Sandstone is the most permeable layer, followed by the Coconino and Windgate sandstones.

(2) **A rechargeable groundwater system**. On the Colorado Plateau, seasonal rainfall is the means by which the sandstone aquifers are recharged, primarily in drainage divide areas where the sandstones are extensively exposed on the surface.

(3) **A free face at which subsurface water can emerge**. Groundwater sapping generally requires some pre-existing scarp (exposure) at which the sapping process can begin, created through either faulting or some other erosional process.

(4) **Some form of structural or lithologic inhomogeneity that locally increases the hydraulic conductivity**. Examples of this include jointing in sandstone, or dikes in volcanic material. Resultant canyons will follow such inhomogeneities in the up-dip direction.

(5) **A means of transporting material away from the scarp face**. This is primarily achieved by fluvial transport. In eroding unconsolidated materials, the transported material makes up about 1-10% of the overall flow, while in consolidated materials, the transported material makes up only about 0.1-1% of the overall flow. This implies that in areas where sandstones form the scarp faces, the volume of water required to create a particular canyon is about 100 to 1000 times the canyon volume.

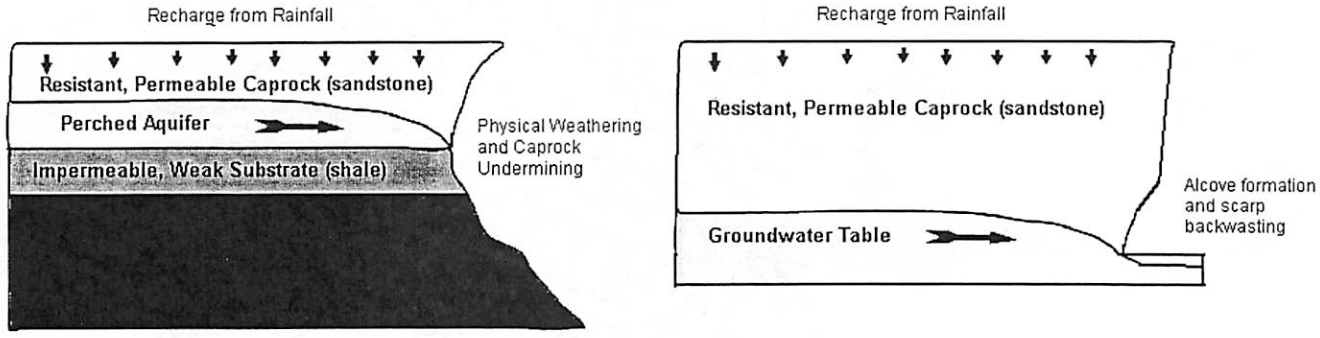

Figure 1: Basic diagram of the requirements for groundwater sapping, in which groundwater seepage at the base of a permeable layer causes undermining and subsequent headward erosion of a scarp face. Two forms are shown: (*left*) a perched aquifer causing erosion of an impermeable "parting" layer (usually shale), and (*right*) alcove formation in a scarp located in a massive sandstone layer, such as in Canyon de Chelly.

Characteristics of Groundwater Sapping Canyons and Networks

The most telling characteristics of sapping canyons are morphological ones. These include:

(1) Valleys that terminate in steep walled headcuts, which are described as cuspate, amphitheater shaped, or U-shaped in form. (See *Figure 2*)

(2) Strong structural control of valley alignment and planform. Valleys grow in the direction of the inherent structural inhomogeneities (joints), and in a generally up-dip direction with regard to the aquifer layer. (See *Figure 3*)

(3) Long main channels with short, stubby tributaries. (See *Figures 3 & 4*)

(4) Hanging tributary channels commonly occur.

(5) Irregular angles of channel junction. These will generally follow the large-scale joint angles for the area, and thus usually display only two or three orientations. (See *Figures 3 & 4*)

(6) Valley widths that remain nearly constant in the downstream direction. (See *Figure 3 & 4*)

(7) Longitudinal profiles of the main channels will generally be straight. (See *Figure 5*)

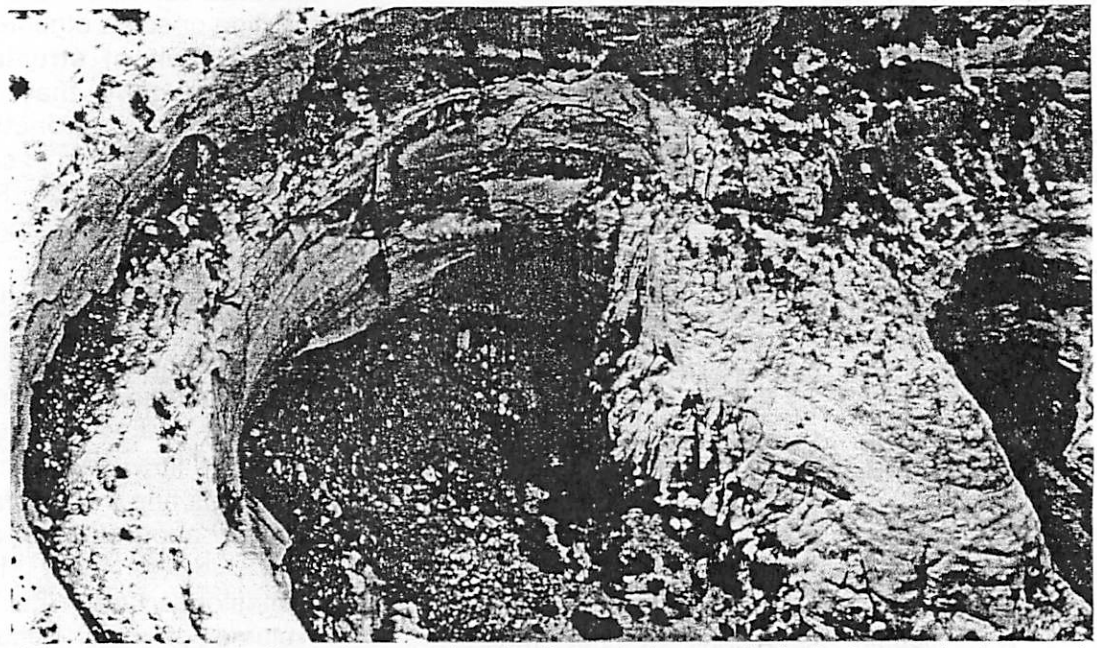

Figure 2: Two amphitheater shaped canyon headwalls and alcoves, typical of groundwater sapping (Navajo Sandstone, Inscription House area, Arizona). Note the sandstone debris from recent rockfalls.

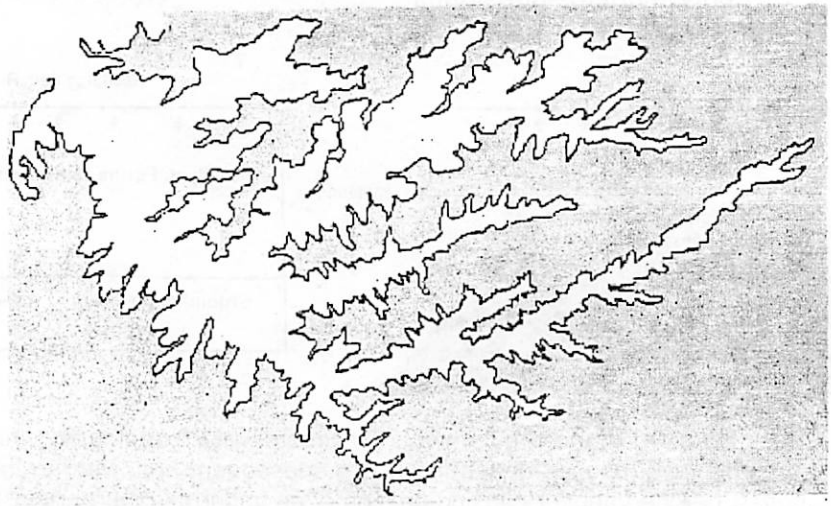

Figure 3: Plan view of a groundwater sapping network in the Navajo Sandstone in New Mexico. Note the inherent structural control as evidenced by the two primary directions of upstream growth.

Canyon Modification by Groundwater Sapping

In canyons which were not initially formed by groundwater sapping, sapping processes can subsequently play an important role in extending and widening the system, beginning with the presence of alcoves and seeps in the canyon walls, moving to the formation of theater-headed, stubby tributaries, and eventually forming separate sapping networks (see *Figure 4*).

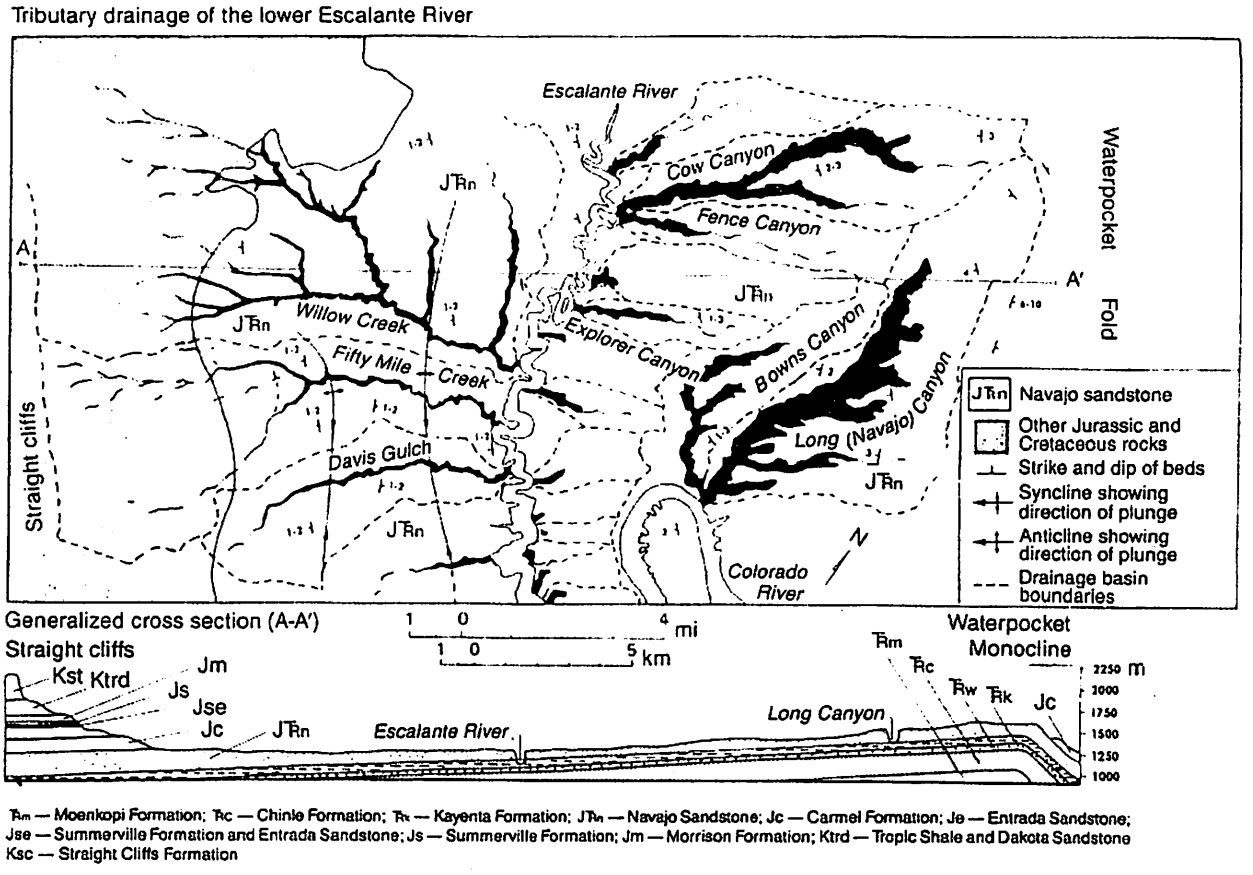

TRm — Moenkopi Formation; TRc — Chinle Formation; TRk — Kayenta Formation; JTRn — Navajo Sandstone; Jc — Carmel Formation; Je — Entrada Sandstone; Jse — Summerville Formation and Entrada Sandstone; Js — Summerville Formation; Jm — Morrison Formation; Ktrd — Tropic Shale and Dakota Sandstone Ksc — Straight Cliffs Formation

Figure 4: Plan view of groundwater sapping channels in the Navajo Sandstone near Glen Canyon, Arizona. The sapping networks occur on the northeastern sides of the Escalante and Colorado river canyons, while runoff drainage systems occur on the southwestern sides --> indicating the up-dip direction of the inherent layers as east-northeast (see accompanying cross-section). Note also that the drainage channels generally end in pointed V-shapes, while the sapping channels generally end in rounded, U-shapes.

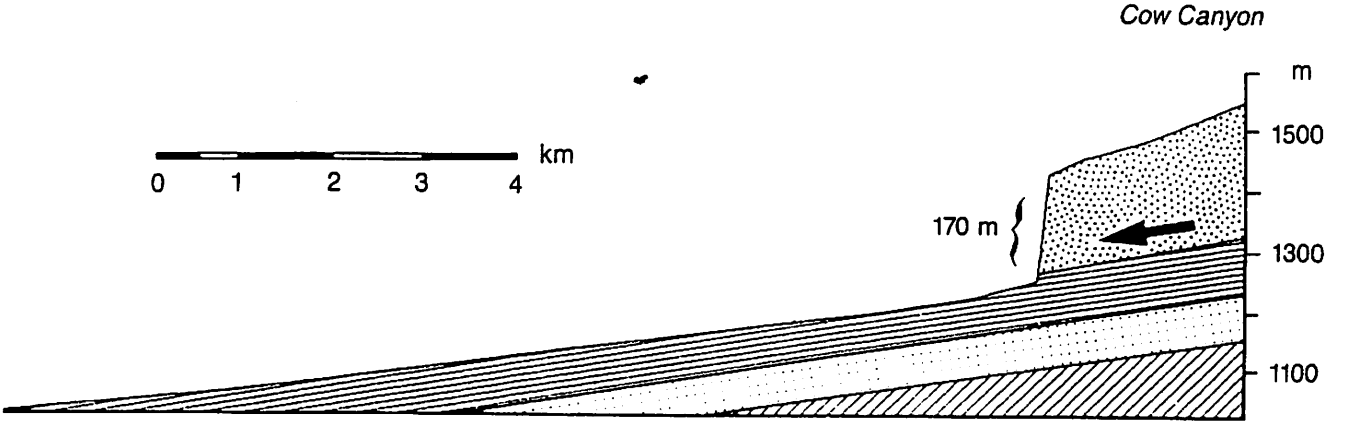

Figure 5: Cross-sectional drawing showing the straight longitudinal profile of Cow Canyon in Arizona, which has a groundwater (spring) flow of about 150-200 liters/minute. This canyon is also shown in plan view in *Figure 4*.

Groundwater Sapping in Canyon de Chelly

Canyon de Chelly and its related canyons were initially formed during the formation of the Defiance Plateau, a 100 mile wide, dome-shaped anticline centered about 20 miles to the south of the canyon system. These canyons are primarily the product of stream down-cutting during this regional Oligocene uplift (24-38 Ma).

Following formation, groundwater sapping has played a role in widening and modifying the canyons, due to the aquifer properties of the massive De Chelly sandstone. Visible geological layers in the canyon include (top to bottom):

(1) Shinarump Conglomerate (Triasic): this is the stream deposited lowest member of the Chinle Formation. This layer forms the resistant caprock of the Defiance Plateau and the Canyon de Chelly area.

(2) De Chelly Sandstone (Permian): a pale, peach-colored rock of desert deposited sandstone with grandious cross-cutting features.

The most noticeable sapping features in this canyon system are the huge alcoves cut into the base of the canyon walls, and indicative of localized groundwater seepage and subsequent undermining of the affected scarp (see *Figure 1*). The further stages of sapping modification, such as stubby, theater-headed tributaries, are also present, but most sapping features in the canyon may be currently inactive (having formed during times of wetter climate).

Canyon de Chelly also displays many groundwater seepage points along its walls, in the form of dark streaks of desert varnish (manganese and iron oxides) below perched, low flow-rate, seasonal water tables. Such desert varnish displays take on the order of 1000 years to form, and therefore indicate very little to no headward erosion of the scarp face at their origins.

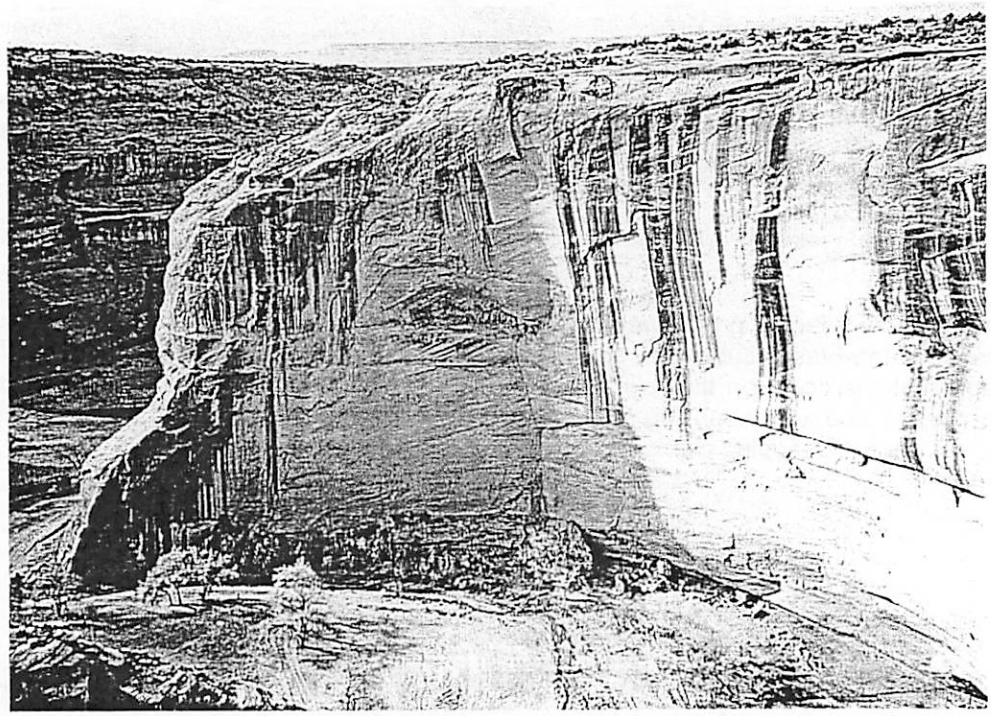

Figure 6: Groundwater seepage in Canyon de Chelly, revealed by the dark streaks of desert varnish. These indicate scarp intersection points with locally perched, low-flow, seasonal water tables (but not sapping). The alcove at the base of the scarp (*lower right*) is indicative of groundwater sapping, although stream undercutting may also have played a role.

References:

Chronic, H. (1983). *Roadside Geology of Arizona*. Missoula, Montana: Mountain Press Pub. Co.

Howard, A.D., Kochel, R.C., & Holt, H.E. (eds.) (1988). *Sapping Features of the Colorado Plateau*, NASA Special Paper 491. Washington: National Aeronautics and Space Administration.

Groundwater Sapping Features on Mars

Oleg Abramov

I. Introduction

Aside from Earth, Mars is the only place in the solar system where groundwater sapping can plausibly occur. The Gamma Ray Spectrometer (GRS) on the Mars Odyssey spacecraft detected large subsurface ice deposits in the polar and subpolar regions. Detailed analysis of the data indicates an ice-rich layer residing beneath an ice-poor upper layer, with the thickness of the upper layer increasing toward the equator. This implies that subsurface ice also exists in the near-equatorial regions at a depth beyond the limit of detection by GRS, and the presence of craters with fluidized ejecta blankets supports this (Fig 2). This subsurface ice can be melted by geothermal activity and the resulting water can flood the surface. One example of this is the outflow channels carved by large catastrophic floods. A more gradual release of water from a subsurface aquifer could have created a long-lived flow and formed a channel by groundwater sapping.

II. Nirgal Vallis – best evidence of groundwater sapping on Mars

Nirgal Vallis is a valley network located in the southern highlands, centered at 29 S, 328 E.

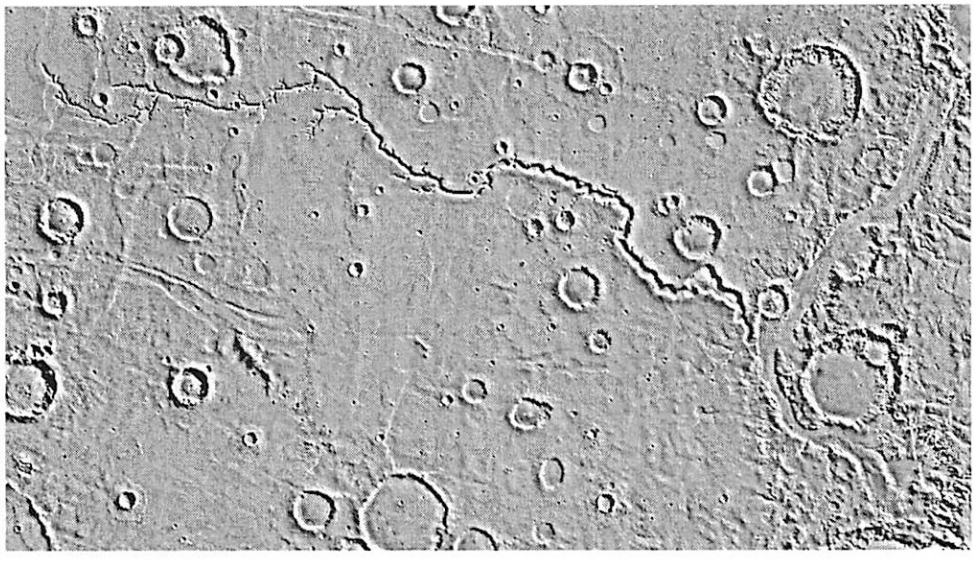

Figure 1. Viking image mosaic of Nirgal Vallis. The channel is ~ 700 km long.

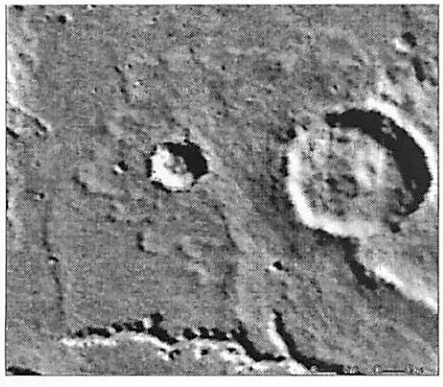

Figure 2. An ~8 km crater with an extensive fluidized ejecta blanket near the source region of Nirgal Vallis. Viking image fragment.

Nirgal Vallis appears to fit all of the morphological criteria for groundwater sapping channels listed in "Sapping Features of the Colorado Plateau":

1) **Amphitheater-shaped valley endpoints**: In the upper reach of Nirgal Vallis almost all tributary valleys terminate in U-shaped alcoves (Fig 3).

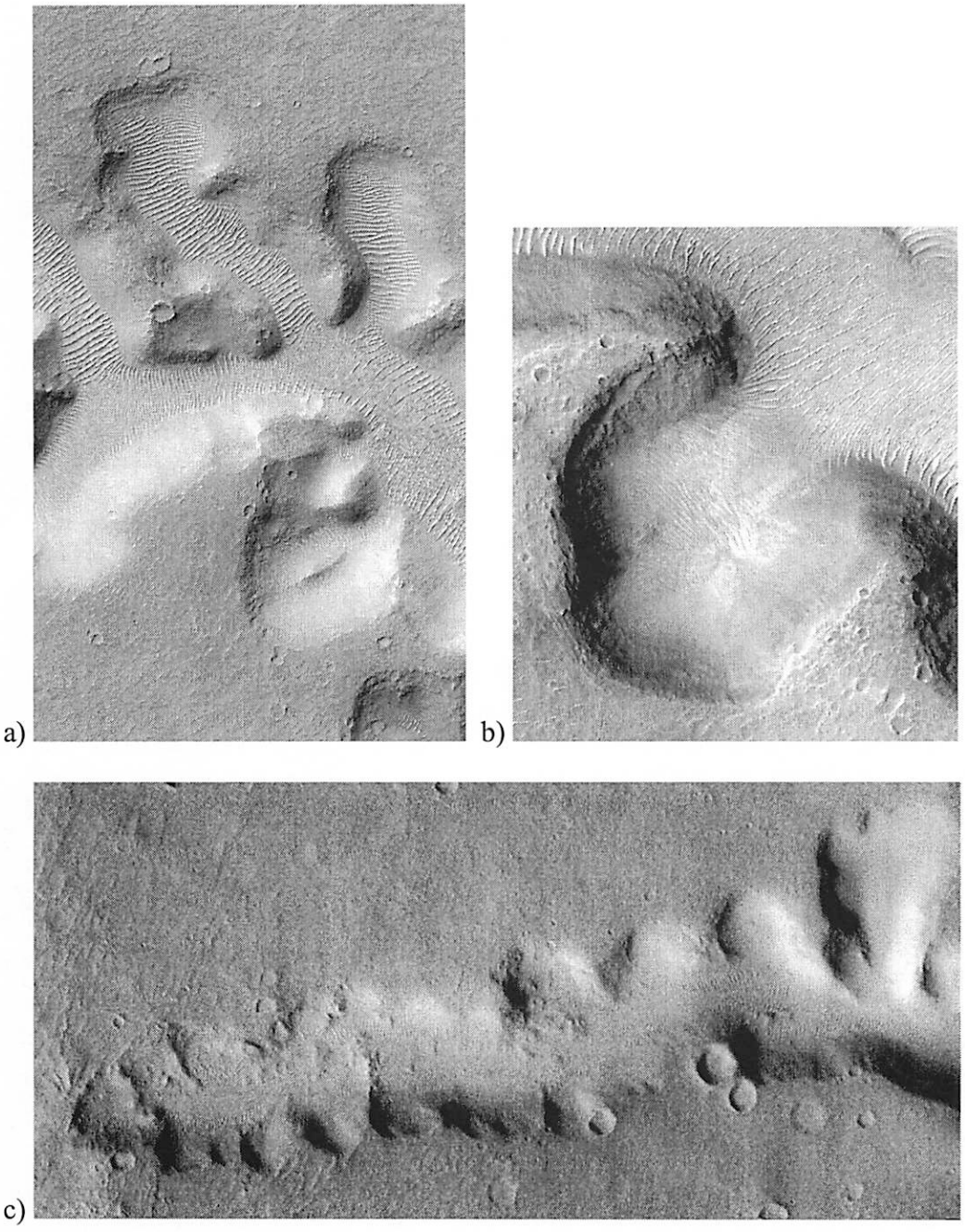

Figure 3. a) Mars Orbital Camera (MOC) image fragment showing short tributary channels, 3.0 m/pixel. b) MOC image fragment showing an amphitheater-shaped alcove, 2.8 m/pixel. c) THEMIS image fragment showing multiple alcoves in a Nirgal Vallis tributary, 18 m/pixel.

2) **Structural control of valley alignment and planform:** Some tributaries of Nirgal Vallis follow visible structural nonhomogenuities (faults, joints), as seen in Fig 4.

3) **Long main valleys with short, stubbly tributaries:** The ~350 km upper reach of Nirgal Vallis, shown in Fig 4, is rich in these types of tributaries.

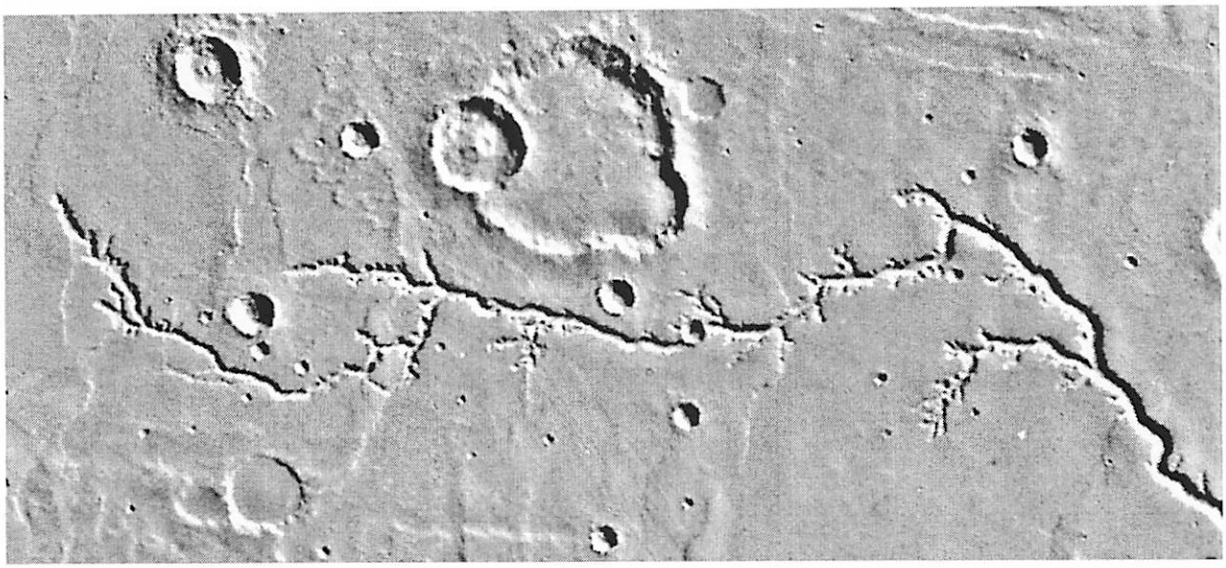

Figure 4. Upper reach of Nirgal Vallis, Viking image mosaic.

4) **Hanging valleys commonly occur**: Hanging tributaries are common in Nirgal Vallis; an example is shown in Fig. 5.

a)

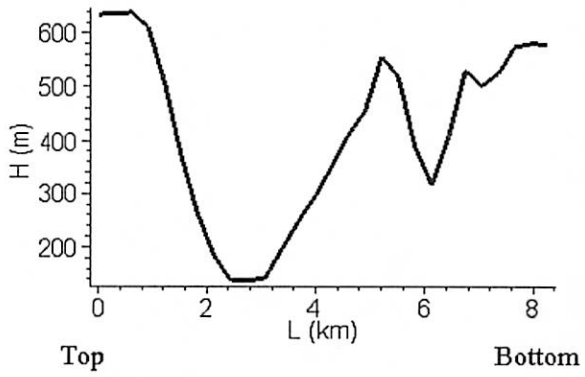

b)

Figure 5. a) MOC image of a portion of Nirgal Vallis. The white line indicates the position of a Mars Orbiter Laser Altimeter (MOLA) track. b) MOLA altimetry profile illustrating a hanging tributary valley.

5) **Valley widths remain nearly constant in the downstream direction:** As seen in Fig. 4, the width of the main channel in the upper reach of Nirgal Vallis remains relatively constant.

5) **Valley widths remain nearly constant in the downstream direction:** As seen in Fig. 4, the width of the main channel in the upper reach of Nirgal Vallis remains relatively constant.

6) **Longitudinal profile of the main channel is generally straight:** The longitudinal profile of Nirgal Vallis (Fig 6) is convex, possibly indicating a decreasing discharge with increasing distance down the reach. This implies that the network primarily received water from the upper portions of the reach and experienced loss of fluid over the course of the reach due to ground seepage or evaporation.

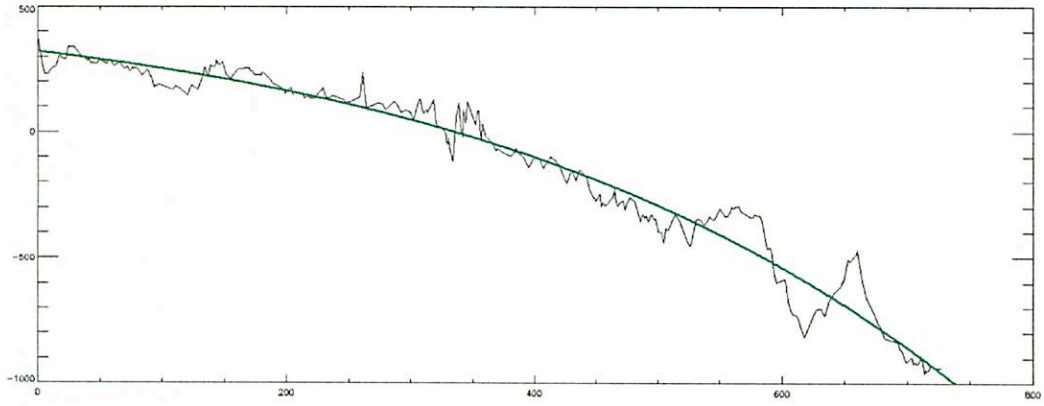

Figure 6. Curve-fit to the Nirgal Vallis longitudinal profile.

7) **The surface dip angle is generally very low (<4°):** The surface dip for the upper reach of Nirgal Vallis is virtually absent (Fig 7).

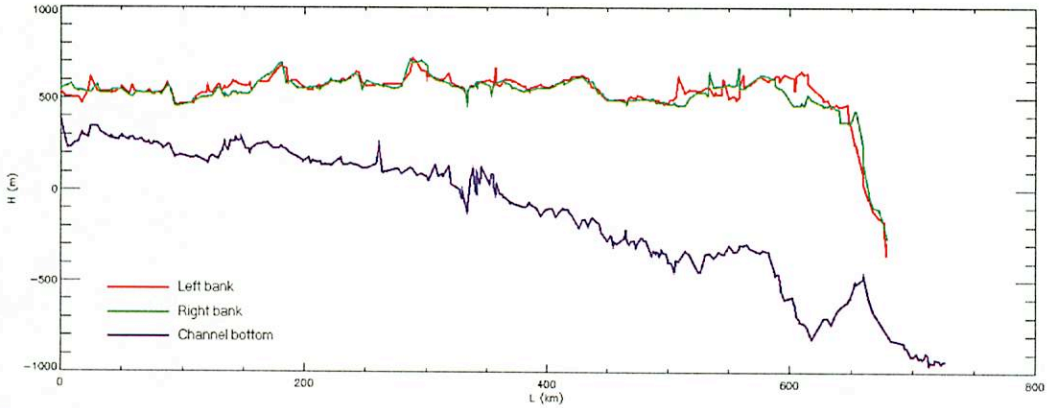

Figure 7. Longitudinal profiles of Nirgal Vallis' bottom and both banks.

III. Implications

Groundwater sapping in general requires a permeable aquifer and a rechargeable groundwater system. The former can be produced from the melting of subsurface ice by geothermal heating, and the latter can plausibly be created by groundwater brought in from surrounding regions.

IV. References

W. V. Boynton, W. C. Feldman, S. W. Squyres, T. H. Prettyman, J. Brückner, L. G. Evans, R. C. Reedy, R. Starr, J. R. Arnold, D. M. Drake, P. A. J. Englert, A. E. Metzger, Igor Mitrofanov, J. I. Trombka, C. d'Uston, H. Wänke, O. Gasnault, D. K. Hamara, D. M. Janes, R. L. Marcialis, S. Maurice, I. Mikheeva, G. J. Taylor, R. Tokar, C. Shinohara, Distribution of Hydrogen in the Near Surface of Mars: Evidence for Subsurface Ice Deposits, *Science*, *297*, 81-85, 2002.

Howard, A. D., Kochel, R. C., and Holt, H. H., eds, Sapping Features of the Colorado Plateau: A Comparative Planetary Geology Field Guide, *NASA Special Publication SP-491*, 108 p, 1998.

Jaumann, R. and D. Reiss, Nirgal Vallis: Evidence for Extensive Sapping, *Lunar Planet. Sci., XXXIII*, abstract 1579, 2002.

CONVECTION IN THE DESERT

Joe Spitale

Introduction

Free convection occurs when denser fluid elements overlie less-dense elements. As the denser parcels fall under the effect of gravity, the less-dense parcels rise to take their place. This is known as a Rayleigh-Taylor instability,

In a clear atmosphere, most of the tropospheric heating occurs at the base, where the surface is heated by sunlight during the day. When a parcel of air is heated near the ground, it expands and rises. As it rises, it cools approximately adiabatically. The parcel will continue to rise only as long as it remains warmer (and therefore less dense) than the surrounding air. Therefore, if the ambient temperature profile is adiabatic or super-adiabatic, parcels will continue to rise and convection will continue. When water vapor is present, latent heat is released as air parcels rise, causing the temperature to decrease more gradually with altitude. In that case, the convection criterion is analogous to the dry case, but the ambient temperature must follow a different altitude profile, known as a moist adiabat[1].

Another way to lift an air parcel is to force it to flow over an obstacle like a mountain. This mechanism is often referred to as forced convection.

Convection in the desert

Near the equator, warm moist air is convected to high altitudes. As that air rises and cools, the water condenses out. In the vicinity of +/- 30 degrees latitude, the dried air descends. Because of this Hadley circulation, we see many deserts at those latitudes on the Earth. Deserts may also be formed in "rain shadows", where moist sea air is dried through forced convection as it flows over mountains.

Precipitation in the desert is often dominated by intense, short-lived convective thunderstorms. Such storms are common during monsoon conditions -- relatively brief periods during which the wind direction is different than that of the prevailing wind. During the monsoon, moisture may be delivered from a source that is upwind during the rest of the year.

Convective thunderstorms form as plumes of moist air rise from near the surface. As the air rises, the relative humidity increases toward saturation. As the air saturates, the water condenses forming droplets or crystals at higher levels. As moisture is removed from the air, the density distribution in the cloud is altered, forming a downdraft at low levels that entrains cool upper-tropospheric air. This downdraft may behave like a density current, spreading out in all directions in a gust front. Eventually, the low-level air loses its bouyancy as it mixes with the cool air of the downdraft and the updraft dissipates. The lifetime of a convective cell is typically of order 1 hour, depending on the speed of the updraft[2].

Mars

There is not enough moisture in the Martian atmosphere for the development of thunderstorms. However, free-convection plumes may be important in the injection of dust into the atmosphere[3], which in turn plays an important role the global circulation[4].

References:

[1] K. A. Emanuel Atmospheric Convection. Oxford University Press, New York, NY 1994
[2] J.W. Chamberlain and D. M. Hunten Theory of Planetary Atmospheres. Academic Press, San Diego, CA 1987
[3] M. Odaka, et al. A numerical study of the Martian atmospheric convection with a two-dimensional anelastic model Earth Planets Space 50, 431-437 1998
[4] Pollack, J. B, et al. Properties and effects of dust particles suspended in the Martian atmosphere JGR 84, 2929-2945 1979

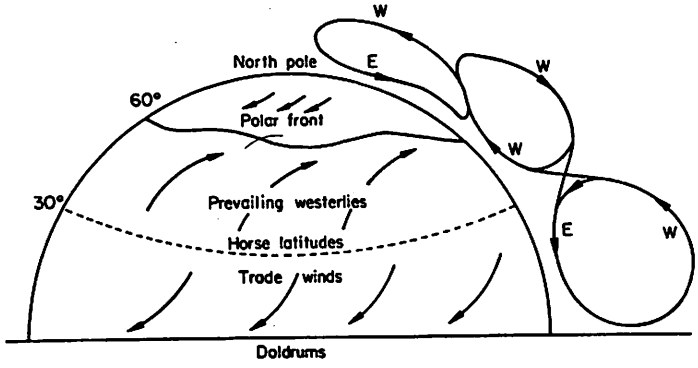

Fig. 2.3 The three-cell circulation scheme, illustrating tropical convection with subsidence in the "horse latitudes," ascent in the zone of polar fronts, and subsidence over the polar cap. The notations W and E refer to the directions from which the prevailing winds arise. [Adapted from C.-G. ROSSBY (1941), *in* "Yearbook of Agriculture, Climate, and Man," G. Hambridge, ed.), pp. 599–655, U.S. Gov. Printing Off., Washington, D.C.]

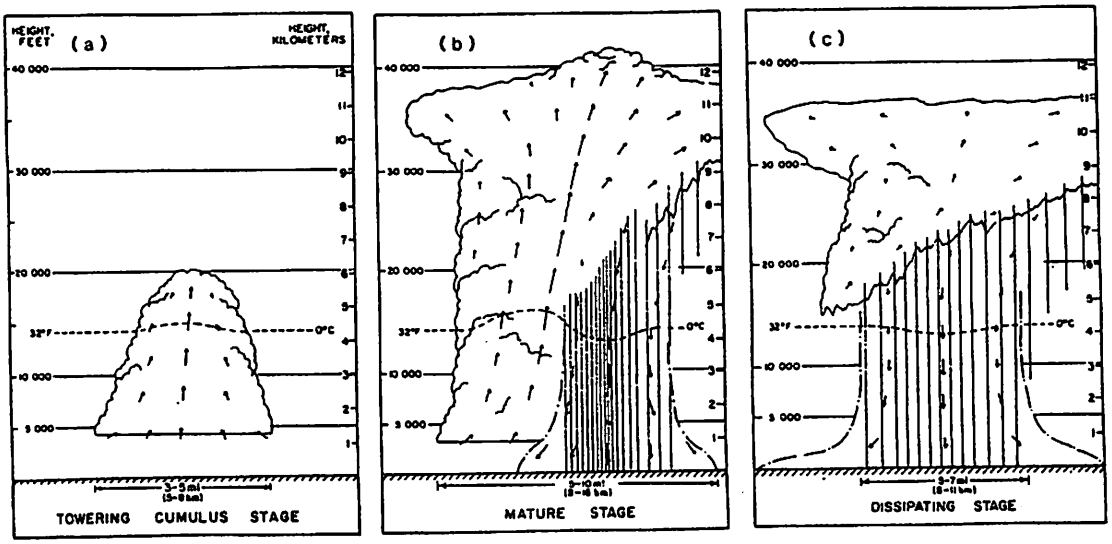

Fig. 9.1 Three stages in the evolution of common convective showers. (a) cumulus stage; (b) mature stage; (c) dissipating stage. Altitude in kilometers on right. Arrows denote air motion; dash-dot lines represent boundary of rain-cooled air. [*From Doswell (1985).*]

IT'S ALL IN A NAME
or, what possessed the town founders to name them the way they did?

Oracle owes its name to a ship in which a local mining man traveled around Cape Horn enroute to the western United States

McMillenville is a ghost silver mining camp. The old community once had 1000 people, not counting the hostile Apaches that waited in the surrounding country. (An attack on the camp was repulsed in 1882.) Production ceased in the mid-1880s.

Show Low was founded in 1875. Two men settled the area, but decided there was only room for one. They played cards and decided the one who could "show low" would remain.

Snowflake isn't just a chilly sledding playground, it was named by combining the names of its two founders, Snow and Flake, in 1878.

Holbrook was named after H. R. Holbrook, the first chief engineer of the Atlantic and Pacific Railroad. This town has been a supply point for ranches and trading posts on the Navajo Reservation.

All tales from Barnes, W. C., Arizona Place Names, University of Arizona General Bulletin no. 2, 1935.